Advances in Applied Mathematics and Mechanics
Adv. Appl. Math. Mech., Vol. **7**, No. 1, pp. 89-115

DOI: 10.4208/aamm.2013.m296
February 2015

Sensitivity Analysis and Computations of the Time Relaxation Model

Monika Neda[1], Fran Pahlevani[2,*] and Jiajia Waters[1]

[1] *Department of Mathematics, University of Nevada, Las Vegas, NV 89154, USA*
[2] *Department of Mathematics, Penn State University-Abington College, PA 19001, USA*

Received 20 July 2013; Accepted (in revised version) 6 August 2014

Abstract. This paper presents a numerical study of the sensitivity of a fluid model known as time relaxation model with respect to variations of the time relaxation coefficient χ. The sensitivity analysis of this model is utilized by the sensitivity equation method and uses the finite element method along with Crank Nicolson method in the fully discretization of the partial differential equations. We present a test case in support of the sensitivity convergence and also provide a numerical comparison between two different strategies of computing the sensitivity, sensitivity equation method and forward finite differences.

AMS subject classifications: 65M60, 65M12, 76D99

Key words: Sensitivity analysis, time relaxation model, Navier-Stokes equations, finite element method.

1 Introduction

Sensitivity investigations have become an important feature in understanding the fluid behavior. A meaningful solution for the Navier-Stokes equations at high Reynolds number requires computations with a fine mesh. This leads to expensive simulations regarding the storage of matrices and running time. Fluid models have been developed in order to avoid these obstacles. As it has been presented in [3], even when a fluid flow model has performed well in practice, the reliability of the approximated flow variables is often not addressed. If the model displays sensitivity to certain parameters, the resulting flow solution is not reliable. To that end, sensitivity analysis techniques provide a measure to compute solution uncertainties due to the variation of the selected parameter and determine a reliable interval for the parameter value. Over the years, there have been studies

*Corresponding author.
Email: monika.neda@unlv.edu (M. Neda), fxp10@psu.edu (F. Pahlevani), wangj16@unlv.nevada.edu (J. Waters)

on the sensitivity of fluid flows in different aspects, [3, 9, 23, 39, 41, 42]. Assessing model error that leads to uncertainty quantification is an important application of sensitivity analysis, see [35, 40] for recent works in this direction. Defining the sensitivity of state variables in a physical system as derivatives of state varaibles with respect to the selected parameter, there are basically two methods of numerically calculating the sensitivities: Forward Finite Difference method (FFD) and Sensitivity Equation Method (SEM). One simply uses finite differences and the other is based on forming an equation for the state variable sensitivity by differentiating the original model equation. In the latter approach, the resulting sensitivity equation is a linear equation and in most cases it is solved in tandem with the model equation when the state variables from the original system appear in the sensitivity equation. SEM is categorized by two different strategies: Continuous Sensitivity Equation Method (CSEM) and Automatic Differentiation Method (ADM). The difference between ADM and CSEM is in the order of operations of discretization and differentiation. CSEM implements differentiation first and then discretization, whereas ADM implements discretization first and then uses differentiation. There have been many works done using ADM, see [24, 25, 28, 29] for some examples. The possibility of combining these two methods is discussed in [12]. While finite difference quotient is easy to compute using a flow solver code, it might not be a reliable technique to compute sensitivites of a fluid model, see [7, 22]. In that aspect, the use of CSEM is preffered to that one of the finite difference, see [6, 39] for a camparison between these two methods in computing sensitivities. For computing flow sensitivity via CSEM, once the flow solver has converged only a linear solve is needed. This is computationally less expensive than running a code for calculating non-linear flow for two different parameter input in the attempt of calculating sensitivity via finite difference quotient. CSEM has been extensively used to compute the sensitivities with respect to different regularization parameters, see [5, 7, 8, 10, 19] for some examples among many others in the literature. This paper explores the sensitivity of a time relaxation type model with respect to a regularization parameter given below.

The governing equations of fluid motion are the Navier Stokes equations,

$$\begin{aligned} &\mathbf{u}_t+\mathbf{u}\cdot\nabla\mathbf{u}+\nabla p-\nu\Delta\mathbf{u}=\mathbf{f} && \text{in } \Omega\times[0,T], \\ &\nabla\cdot\mathbf{u}=0 && \text{in } \Omega\times[0,T], \end{aligned}$$

where $\mathbf{u}$ and p represent velocity vector and pressure respectively, ν represents the viscosity and $\mathbf{f}$ represents the body force. Time Relaxation model (TRM) was introduced by Stolz, Adams and Kleiser [17]. The model was computationally tested on compressible flows with shocks and on turbulent flows [1, 2, 17], i.e., on the aerodynamic noise [20]. A continuous finite element analysis for the model along with numerical results can be found in [17], while a discontinuous finite element analysis can be found in [36]. Preliminary sensitivity computations can be found in [37]. In [38] a computational study have been published of the Leray-α model with respect to the filter width. This model applies a regularization to the non-linear term in NSE in the form of $\overline{\mathbf{u}}\cdot\nabla\mathbf{u}$, where $\overline{\mathbf{u}}$ is calculated from the differential filter given in Eq. (1.2). TRM consists of the Navier-Stokes equations with an addition of a stabilization term to the momentum equation. Thus, TRM is defined by

$$\mathbf{u}_t+\mathbf{u}\cdot\nabla\mathbf{u}+\nabla p-\nu\Delta\mathbf{u}+\chi(\mathbf{u}-G_N\overline{\mathbf{u}})=\mathbf{f} \qquad \text{in } \Omega\times[0,T], \tag{1.1a}$$

$$\nabla\cdot\mathbf{u}=0 \qquad \text{on } \Omega\times[0,T]. \tag{1.1b}$$

Here, $\overline{\mathbf{u}}$ represents an averaged function of $\mathbf{u}$ by filter width δ, with notation $\overline{\mathbf{u}}=G\mathbf{u}$, that satisfies

$$-\delta^2\Delta\overline{\mathbf{u}}+\overline{\mathbf{u}}=\mathbf{u} \qquad \text{in } \Omega, \tag{1.2a}$$

$$\overline{\mathbf{u}}=0 \qquad \text{on } \partial\Omega. \tag{1.2b}$$

G_N represents the continuous van Cittert deconvolution operator and it is defined as, [33],

$$G_N\mathbf{u}:=\sum_{n=0}^{N}(I-G)^n\mathbf{u}.$$

For order of deconvolution $N=0$ and $N=1$, we have: $G_0\mathbf{u}=\mathbf{u}$, $G_1\mathbf{u}=2\mathbf{u}-\overline{\mathbf{u}}$. Higher order of deconvolution increases accuracy since $\mathbf{u}-G_N\overline{\mathbf{u}}=\mathcal{O}(\delta^{2N+2})$, however it also requires additional computational time [15]. Herein, the studies are carried out for the fundamental case, i.e., order of deconvolution $N=0$. The action of the term $\chi(\mathbf{u}-G_N\overline{\mathbf{u}})$ is to drive fluctuations lower than $\mathcal{O}(\delta)$ to zero as $t\to\infty$ while maintaining the accuracy of the model's solution $\mathbf{u}$. Thus, this term reduces the number of degrees of freedom per time step in simulation. Parameter χ represents the time relaxation coefficient and has units $1/time$. The value of this parameter specifies how strongly the growth of fluctuations are truncated. The study of time relaxation operator presented in [34] concludes that $\chi=\mathcal{O}(\delta^{-2/3})$ for turbulent flows. Since different values of χ will cause different responses of the flow, it is natural to explore how the change of the flow will be affected by altering this parameter. In this paper we obtain sensitivity computations using both FFD and SEM. The sensitivity using FFD is obtained by the formula

$$\frac{\mathbf{u}(\chi+\Delta\chi)-\mathbf{u}(\chi)}{\Delta\chi} \tag{1.3}$$

by numerically computing $\mathbf{u}$ from (1.1b) for two different time relaxation parameters, $\chi+\Delta\chi$ and χ.

Sensitivity of the solution $(\mathbf{u},p)$ with respect to χ for the SEM is obtained by differentiating (1.1b) (with $N=0$) with respect to χ,

$$\mathbf{s}_t+\mathbf{u}\cdot\nabla\mathbf{s}+\mathbf{s}\cdot\nabla\mathbf{u}+\nabla r-\nu\Delta\mathbf{s}+(\mathbf{u}-\overline{\mathbf{u}})+\chi(\mathbf{s}-\mathbf{w})=0 \qquad \text{in } \times[0,T], \tag{1.4a}$$

$$\nabla\cdot\mathbf{s}=0 \qquad \text{in } \Omega\times[0,T], \tag{1.4b}$$

$$\mathbf{s}=0 \qquad \text{on } \partial\Omega\times[0,T], \tag{1.4c}$$

where $\mathbf{s}=\partial\mathbf{u}/\partial\chi$, $r=\partial p/\partial\chi$ and $\mathbf{w}=\partial\overline{u}/\partial\chi$. Here, $\mathbf{w}$ satisfies the following filtering equation,

$$-\delta^2\Delta\mathbf{w}+\mathbf{w}=\mathbf{s} \qquad \text{in } \Omega, \tag{1.5a}$$

$$\mathbf{w}=0 \qquad \text{on } \partial\Omega. \tag{1.5b}$$

As we see in (1.4), $\mathbf{u}$ appears in the sensitivity equation. Hence, in order to obtain the solution for (1.4) we need to couple (1.1b) with (1.4).

2 Finite element preliminaries

This section presents the finite element notation, preliminary results, and the finite element schemes in order to numerically solve (1.1b) and (1.4). The $L^2(\Omega)$ norm and inner product will be denoted by $\|\cdot\|$ and $(\cdot,\cdot)$. Likewise, the $L^p(\Omega)$ norms and the Sobolev $W_p^k(\Omega)$ norms are denoted by $\|\cdot\|_{L^p}$ and $\|\cdot\|_{W_p^k}$, respectively. For the semi-norm in $W_p^k(\Omega)$ we use $|\cdot|_{W_p^k}$. H^k is used to represent the Sobolev space W_2^k, and $\|\cdot\|_k$ denotes the norm in H^k. For functions $v(\mathbf{x},t)$ defined on the entire time interval $(0,T)$, we define

$$\|v\|_{\infty,k}:=\sup_{0<t<T}\|v(t,\cdot)\|_k \quad \text{and} \quad \|v\|_{m,k}:=\Big(\int_0^T\|v(t,\cdot)\|_k^m dt\Big)^{1/m}.$$

The velocity and pressure finite element spaces (X^h,Q^h) are defined respectively,

$$X^h\subset X=H_0^1(\Omega):=\{v\in H^1(\Omega):\ v|_{\partial\Omega}=0\},$$

$$Q^h\subset Q=L_0^2(\Omega):=\Big\{q\in L^2(\Omega)\Big|\int_\Omega q=0\Big\},$$

and the space of discretely divergence free velocity is

$$V_h=\big\{\mathbf{v}\in X_h:(q,\nabla\cdot\mathbf{v})=0,\ \forall q\in Q^h\big\}.$$

We assume that the spaces X^h, Q^h satisfy the discrete inf-sup condition. We denote the dual space of X as X', with norm $\|\cdot\|_{-1}$. Also, bilinear $a(\cdot,\cdot):X\times X\to\mathrm{IR}$ and trilinear $b^*(\cdot,\cdot,\cdot):X\times X\times X\to\mathrm{IR}$ forms are defined as,

$$a(\mathbf{u},\mathbf{v}):=(\nabla\mathbf{u},\nabla\mathbf{v}),$$

$$b^*(\mathbf{u},\mathbf{v},\mathbf{w}):=\frac{1}{2}(\mathbf{u}\cdot\nabla\mathbf{v},\mathbf{w})-\frac{1}{2}(\mathbf{u}\cdot\nabla\mathbf{w},\mathbf{v}).$$

Lemma 2.1 (see [30,31]). *For $\mathbf{u},\mathbf{v},\mathbf{w}\in X$, and also $\mathbf{v}\in L^\infty(\Omega)$ for the first estimate, the trilinear term $b^*(\mathbf{u},\mathbf{v},\mathbf{w})$ can be bounded by*

$$b^*(\mathbf{u},\mathbf{v},\mathbf{w})\le C(\Omega)\|\mathbf{u}\|^{\frac{1}{2}}\|\nabla\mathbf{u}\|^{\frac{1}{2}}\|\nabla\mathbf{v}\|\|\nabla\mathbf{w}\|,$$

$$b^*(\mathbf{u},\mathbf{v},\mathbf{w})\le C(\Omega)\|\nabla\mathbf{u}\|\|\nabla\mathbf{v}\|\|\nabla\mathbf{w}\|.$$

Let Δt be the step size for t so that $t_n = n\Delta t$, $n=0,1,2,\cdots,N_T$, with $T := N_T \Delta t$. We define the following additional norms:

$$|||v|||_{\infty,k} := \max_{0\le n\le N_T} \|v^n\|_k, \qquad |||v_{1/2}|||_{\infty,k} := \max_{1\le n\le N_T} \|v^{n-1/2}\|_k,$$
$$|||v|||_{m,k} := \Big(\sum_{n=0}^{N_T} \|v^n\|_k^m \Delta t\Big)^{1/m}, \qquad |||v_{1/2}|||_{m,k} := \Big(\sum_{n=1}^{N_T} \|v^{n-1/2}\|_k^m \Delta t\Big)^{1/m}.$$

We also use the following approximation properties in the finite element analysis, [13]:

$$\inf_{\mathbf{v}\in X^h} \|\mathbf{u}-\mathbf{v}\| \le Ch^{k+1}\|\mathbf{u}\|_{k+1}, \qquad \mathbf{u}\in H^{k+1}(\Omega)^{\acute{d}}, \tag{2.1a}$$
$$\inf_{\mathbf{v}\in X^h} \|\mathbf{u}-\mathbf{v}\|_1 \le Ch^{k}\|\mathbf{u}\|_{k+1}, \qquad \mathbf{u}\in H^{k+1}(\Omega)^{\acute{d}}, \tag{2.1b}$$
$$\inf_{r\in Q^h} \|p-r\| \le Ch^{s+1}\|p\|_{s+1}, \qquad p\in H^{s+1}(\Omega). \tag{2.1c}$$

The following theorem is about bounds for the filtered quantities that are applied in the finite element analysis.

Theorem 2.1. *For $v\in X$, we have the following bounds,*

$$\|\overline{\mathbf{v}}^h\| \le \|\mathbf{v}\| \quad \textit{and} \quad \|\nabla\overline{\mathbf{v}}^h\| \le \|\nabla\mathbf{v}\|.$$

Proof. It can be found in [32]. □

The Gronwall's inequality is known to have an important role in the analysis of differential sysytems of variuos kind. In this study, we apply the discrete Gronwall's lemma given in the following statement.

Lemma 2.2 (Discrete Gronwall's Lemma, see [27])**.** *Let Δt, H, and a_n, b_n, c_n, γ_n (for integers $n\ge 0$) be nonnegative numbers such that*

$$a_l + \Delta t\sum_{n=0}^{l} b_n \le \Delta t\sum_{n=0}^{l}\gamma_n a_n + \Delta t\sum_{n=0}^{l} c_n + H \quad \textit{for} \ \ l\ge 0.$$

Suppose that $\Delta t\gamma_n < 1$, for all n, and set $\sigma_n = (1-\Delta t\gamma_n)^{-1}$. Then,

$$a_l + \Delta t\sum_{n=0}^{l} b_n \le \exp\Big(\Delta t\sum_{n=0}^{l}\sigma_n\gamma_n\Big)\Big\{\Delta t\sum_{n=0}^{l} c_n + H\Big\} \quad \textit{for} \ \ l\ge 0.$$

3 Variational formulation and numerical scheme

The variational formulations of TRM given by (1.1b)-(1.2) and SEM by (1.4)-(1.5) using suitable set of test functions from X and Q are respectively given as,

$$
\begin{aligned}
&(\mathbf{u}_t,\mathbf{v})+\nu a(\mathbf{u},\mathbf{v})+ b^*(\mathbf{u},\mathbf{u},\mathbf{v})-(p,\nabla\cdot\mathbf{v})+\chi(\mathbf{u}-\overline{\mathbf{u}},\mathbf{v})=(\mathbf{f},\mathbf{v}), && \forall\mathbf{v}\in X, && (3.1a)\\
&(\nabla\cdot\mathbf{u},q)=0, && \forall q\in Q, && (3.1b)\\
&\delta^2(\nabla\overline{\mathbf{u}},\nabla\mathbf{v})+(\overline{\mathbf{u}},\mathbf{v})=(\mathbf{u},\mathbf{v}), && \forall\mathbf{v}\in X, && (3.1c)
\end{aligned}
$$

and

$$
\begin{aligned}
&(\mathbf{s}_t,\mathbf{v})+\nu a(\mathbf{s},\mathbf{v})+b^*(\mathbf{s},\mathbf{u},\mathbf{v})+b^*(\mathbf{u},\mathbf{s},\mathbf{v})-(r,\nabla\cdot\mathbf{v})+(\mathbf{u}-\overline{\mathbf{u}},\mathbf{v})\\
&\qquad+\chi(\mathbf{s}-\mathbf{w},\mathbf{v})=0, && \forall\mathbf{v}\in X, && (3.2a)\\
&(\nabla\cdot\mathbf{s},q)=0, && \forall q\in Q, && (3.2b)\\
&\delta^2(\nabla\mathbf{w},\nabla\mathbf{v})+(\mathbf{w},\mathbf{v})=(\mathbf{s},\mathbf{v}), && \forall\mathbf{v}\in X. && (3.2c)
\end{aligned}
$$

The Crank-Nicolson method, which is second order approximation in time, is used for the discretization of the time derivative. For notational clarity, in the discussion of the Crank-Nicolson temporal discretization, we let $v(t^{n+1/2})=v((t^{n+1}+t^n)/2)$ for the continuous variable and $v^{n+1/2}=(v^{n+1}+v^n)/2$ for both, continuous and discrete variables. Thus, we obtain the following discretized finite element variational formulations.

Given (X^h,Q^h), end-time $T>0$, the time step is chosen $\Delta t<T=M\Delta t$, find the approximated TRM solution $(\mathbf{u}_h^{n+1},p_h^{n+1})\in(X^h,Q^h)$, for $n=0,1,2,\cdots,M-1$, satisfying:

$$
\begin{aligned}
&\frac{1}{\Delta t}(\mathbf{u}_h^{n+1}-\mathbf{u}_h^n,\mathbf{v}_h)+\nu a(\mathbf{u}_h^{n+1/2},\mathbf{v}_h)+b^*(\mathbf{u}_h^{n+1/2},\mathbf{u}_h^{n+1/2},\mathbf{v}_h)\\
&\quad-(p_h^{n+1},\nabla\cdot\mathbf{v}_h)+\chi(\mathbf{u}_h^{n+1/2}-\overline{\mathbf{u}}_h{}^{n+1/2},\mathbf{v}_h)=(\mathbf{f}^{n+1/2},\mathbf{v}_h), && \forall\mathbf{v}_h\in X^h, && (3.3a)\\
&(\nabla\cdot\mathbf{u}_h^{n+1},q_h)=0, && \forall q_h\in Q^h, && (3.3b)\\
&\delta^2(\nabla\overline{\mathbf{u}}_h{}^{n+1},\nabla\mathbf{v}_h)+(\overline{\mathbf{u}}_h{}^{n+1},\mathbf{v}_h)=(\mathbf{u}_h^{n+1},\mathbf{v}_h), && \forall\mathbf{v}_h\in X^h, && (3.3c)
\end{aligned}
$$

and the sensitivity solution $(\mathbf{s}_h^{n+1},v_h^{n+1})\in(X^h,Q^h)$, for $n=0,1,2,\cdots,M-1$, satisfying:

$$
\begin{aligned}
&\frac{1}{\Delta t}(\mathbf{s}_h^{n+1}-\mathbf{s}_h^n,\mathbf{v}_h)+\nu a(\mathbf{s}_h^{n+1/2},\mathbf{v}_h)+b^*(\mathbf{s}_h^{n+1/2},\mathbf{u}_h^{n+1/2},\mathbf{v}_h)+b^*(\mathbf{u}_h^{n+1/2},\mathbf{s}_h^{n+1/2},\mathbf{v}_h)\\
&\quad-(r_h^{n+1},\nabla\cdot\mathbf{v}_h)+(\mathbf{u}_h^{n+1/2}-\overline{\mathbf{u}}_h^{h^{n+1/2}},\mathbf{v}_h)+\chi(\mathbf{s}_h^{n+1/2}-\mathbf{w}_h^{n+1/2},\mathbf{v}_h)=0, && \forall\mathbf{v}_h\in X^h, && (3.4a)\\
&(\nabla\cdot\mathbf{s}_h^{n+1},q_h)=0, && \forall q_h\in Q^h, && (3.4b)\\
&\delta^2(\nabla\mathbf{w}_h^{n+1},\nabla v_h)+(\mathbf{w}_h^{n+1},\mathbf{v}_h)=(\mathbf{s}_h^{n+1},\mathbf{v}_h), && \forall\mathbf{v}_h\in X^h. && (3.4c)
\end{aligned}
$$

Eqs. (3.3a)-(3.3c) and (3.4a)-(3.4c) can be rewritten equivalently in the space V^h as given below.

Find $\mathbf{u}_h^{n+1}\in V^h$, for $n=0,1,2,\cdots,M-1$, satisfying:

$$\begin{aligned}&\frac{1}{\Delta t}(\mathbf{u}_h^{n+1}-\mathbf{u}_h^n,\mathbf{v}_h)+\nu a(\mathbf{u}_h^{n+1/2},\mathbf{v}_h)+b^*(\mathbf{u}_h^{n+1/2},\mathbf{u}_h^{n+1/2},\mathbf{v}_h)\\&\quad+\chi(\mathbf{u}_h^{n+1/2}-\overline{\mathbf{u}}_h^{h\,n+1/2},\mathbf{v}_h)=(\mathbf{f}^{n+1/2},\mathbf{v}_h), &&\forall\mathbf{v}_h\in V^h, \quad (3.5a)\\&\delta^2(\nabla\overline{\mathbf{u}}_h^{h\,n+1},\nabla\mathbf{v}_h)+(\overline{\mathbf{u}}_h^{h\,n+1},\mathbf{v}_h)=(\mathbf{u}_h^{n+1},\mathbf{v}_h), &&\forall\mathbf{v}_h\in V^h, \quad (3.5b)\end{aligned}$$

and for the sensitivity solution, find $\mathbf{s}_h^{n+1}\in V^h$, for $n=0,1,2,\cdots,M-1$, satisfying:

$$\begin{aligned}&\frac{1}{\Delta t}(\mathbf{s}_h^{n+1}-\mathbf{s}_h^n,\mathbf{v}_h)+\nu a(\mathbf{s}_h^{n+1/2},\mathbf{v}_h)+b^*(\mathbf{s}_h^{n+1/2},\mathbf{u}_h^{n+1/2},\mathbf{v}_h)+b^*(\mathbf{u}_h^{n+1/2},\mathbf{s}_h^{n+1/2},\mathbf{v}_h)\\&\quad+(\mathbf{u}_h^{n+1/2}-\overline{\mathbf{u}}_h^{h\,n+1/2},\mathbf{v}_h)+\chi(\mathbf{s}_h^{n+1/2}-\mathbf{w}_h^{n+1/2},\mathbf{v}_h)=0, &&\forall\mathbf{v}_h\in V^h, \quad (3.6a)\\&\delta^2(\nabla\mathbf{w}_h^{n+1},\nabla v_h)+(\mathbf{w}_h^{n+1},\mathbf{v}_h)=(\mathbf{s}_h^{n+1},\mathbf{v}_h), &&\forall\mathbf{v}_h\in V^h. \quad (3.6b)\end{aligned}$$

4 Finite element analysis

Herein, we derive an a priori sensitivity estimate and sensitivity error estimates for the above given finite element schemes. We use C to denote a generic constant independent of h and Δt, throughout this section.

4.1 A priori sensitivity estimate

First, we recall a lemma proved in [17] that gives the stability estimate and the existence of the finite element solution of TRM.

Lemma 4.1. *For the approximation scheme* (3.5a)-(3.5b) *we have that a solution* $\mathbf{u}_h^{n+1}$, *with* $n=0,\cdots,M-1$, *exists at each iteration and, for* $\Delta t<1$, *satisfies the following a priori bound*

$$\|\mathbf{u}_h^{n+1}\|^2+2\Delta t\nu\sum_{l=0}^{n}\|\nabla\mathbf{u}_h^{n+1/2}\|^2\le C\big(|||\mathbf{f}|||_{2,0}^2+\|\mathbf{u}_h^0\|^2\big). \tag{4.1}$$

Next, we present the same results for the finite element sensitivity solution.

Lemma 4.2. *For the approximation scheme* (3.6a)-(3.6b) *we have that a solution* $\mathbf{s}_h^{n+1}$, *with* $n=0,\cdots,M-1$, *exists at each iteration and, for* $\Delta t<C\nu^{-3}(|||\nabla(\mathbf{u}-\mathbf{u}_h)|||_{4,0}^4+|||\nabla\mathbf{u}|||_{4,0}^4)$, *(with* $\mathbf{u}$ *being a strong solution of* (1.1b)*), satisfies the following a priori bound*

$$\|\mathbf{s}_h^{n+1}\|^2+2\nu\Delta t\sum_{l=0}^{n}\|\nabla\mathbf{s}_h^{n+1/2}\|^2\le C\nu^{-2}\delta^2\big(|||\mathbf{f}|||_{2,0}^2+\|\mathbf{u}_h^0\|^2\big). \tag{4.2}$$

Proof. To obtain the a priori estimate, we set $\mathbf{v}_h=\mathbf{s}_h^{n+1/2}$ in (3.6a), and that gives

$$\frac{1}{2\Delta t}\big(\|\mathbf{s}_h^{n+1}\|^2-\|\mathbf{s}_h^n\|^2\big)+\nu\|\nabla\mathbf{s}_h^{n+1/2}\|^2+b^*(\mathbf{s}_h^{n+1/2},\mathbf{u}_h^{n+1/2},\mathbf{s}_h^{n+1/2})$$
$$+b^*(\mathbf{u}_h^{n+1/2},\mathbf{s}_h^{n+1/2},\mathbf{s}_h^{n+1/2})+(\mathbf{u}_h^{n+1/2}-\overline{\mathbf{u}}_h^{h^{n+1/2}},\mathbf{s}_h^{n+1/2})+\chi(\mathbf{s}_h^{n+1/2}-\mathbf{w}_h^{n+1/2},\mathbf{s}_h^{n+1/2})=0.$$

Noting that $b^*(\mathbf{u}_h^{n+1/2},\mathbf{s}_h^{n+1/2},\mathbf{s}_h^{n+1/2})=0$ and that $\chi(\mathbf{s}_h^{n+1/2}-\mathbf{w}_h^{n+1/2},\mathbf{s}_h^{n+1/2})\geq 0$ (using the positivity of the operator $I-G$ from [15]) we obtain

$$\begin{aligned}&\frac{1}{2\Delta t}\big(\|\mathbf{s}_h^{n+1}\|^2-\|\mathbf{s}_h^n\|^2\big)+\nu\|\nabla\mathbf{s}_h^{n+1/2}\|^2\\ \leq&|b^*(\mathbf{s}_h^{n+1/2},\mathbf{u}_h^{n+1/2},\mathbf{s}_h^{n+1/2})|+|(\mathbf{u}_h^{n+1/2}-\overline{\mathbf{u}}_h^{n+1/2},\mathbf{s}_h^{n+1/2})|.\end{aligned}$$

Next, we bound the two terms on the RHS.

$$\begin{aligned}&|b^*(\mathbf{s}_h^{n+1/2},\mathbf{u}_h^{n+1/2},\mathbf{s}_h^{n+1/2})|\\ \leq&|b^*(\mathbf{s}_h^{n+1/2},\mathbf{u}^{n+1/2}-\mathbf{u}_h^{n+1/2},\mathbf{s}_h^{n+1/2})|+|b^*(\mathbf{s}_h^{n+1/2},\mathbf{u}^{n+1/2},\mathbf{s}_h^{n+1/2})|\\ \leq&\sqrt{\|\mathbf{s}_h^{n+1/2}\|\|\nabla\mathbf{s}_h^{n+1/2}\|}\,\|\nabla(\mathbf{u}^{n+1/2}-\mathbf{u}_h^{n+1/2})\|\|\nabla\mathbf{s}_h^{n+1/2}\|\\ &+\sqrt{\|\mathbf{s}_h^{n+1/2}\|\|\nabla\mathbf{s}_h^{n+1/2}\|}\,\|\nabla\mathbf{u}^{n+1/2}\|\|\nabla\mathbf{s}_h^{n+1/2}\|\\ \leq&\frac{\nu}{3}\|\nabla\mathbf{s}_h^{n+1/2}\|^2+C\nu^3\big(\|\nabla(\mathbf{u}^{n+1/2}-\mathbf{u}_h^{n+1/2})\|^4+\|\nabla\mathbf{u}^{n+1/2}\|^4\big)\|\mathbf{s}_h^{n+1/2}\|^2.\end{aligned}\tag{4.3}$$

To bound the second term, we start by deriving the following bound. Evaluating (3.3c) at time t^{n+1} and t^n, and taking its average, we have

$$\delta^2(\nabla\overline{\mathbf{u}}_h{}^{n+1/2},\nabla\mathbf{v}_h)+(\overline{\mathbf{u}}_h{}^{n+1/2},\mathbf{v}_h)=(\overline{\mathbf{u}}_h^{n+1/2},\mathbf{v}_h),\quad\forall\mathbf{v}_h\in X^h,$$

and by rearranging the terms we obtain

$$(\overline{\mathbf{u}}_h^{n+1/2}-\overline{\mathbf{u}}_h{}^{n+1/2},\mathbf{v}_h)=\delta^2(\nabla\overline{\mathbf{u}}_h{}^{n+1/2},\nabla\mathbf{v}_h),\quad\forall\mathbf{v}_h\in X^h.$$

Letting $\mathbf{v}_h=\overline{\mathbf{u}}_h^{n+1/2}-\overline{\mathbf{u}}_h{}^{n+1/2}$, and using Theorem 2.1, we have

$$\begin{aligned}\|\overline{\mathbf{u}}_h^{n+1/2}-\overline{\mathbf{u}}_h{}^{n+1/2}\|^2\leq&\delta^2\|\nabla\overline{\mathbf{u}}_h{}^{n+1/2}\|\|\nabla(\overline{\mathbf{u}}_h^{n+1/2}-\overline{\mathbf{u}}_h{}^{n+1/2})\|\\ \leq&C\delta\|\nabla\mathbf{u}_h^{n+1/2}\|\|\overline{\mathbf{u}}_h^{n+1/2}-\overline{\mathbf{u}}_h{}^{n+1/2}\|\\ \leq&\frac{1}{2}\|\overline{\mathbf{u}}_h^{n+1/2}-\overline{\mathbf{u}}_h{}^{n+1/2}\|^2+c\delta^2\|\nabla\mathbf{u}_h^{n+1/2}\|^2.\end{aligned}$$

Thus

$$\|\overline{\mathbf{u}}_h^{n+1/2}-\overline{\mathbf{u}}_h{}^{n+1/2}\|^2\leq C\delta^2\|\nabla\mathbf{u}_h^{n+1/2}\|^2.\tag{4.4}$$

Using (4.4), we bound the second term as

$$\begin{aligned}
&|(\mathbf{u}_h^{n+1/2}-\overline{\mathbf{u}}_h{}^{n+1/2},\mathbf{s}_h^{n+1/2})|\le\|\mathbf{u}_h^{n+1/2}-\overline{\mathbf{u}}_h{}^{n+1/2}\|\|\mathbf{s}_h^{n+1/2}\|\\
\le&\frac{\nu}{6}\|\mathbf{s}_h^{n+1/2}\|^2+C\nu^{-1}\|\mathbf{u}_h^{n+1/2}-\overline{\mathbf{u}}_h{}^{n+1/2}\|^2\\
\le&\frac{\nu}{6}\|\mathbf{s}_h^{n+1/2}\|^2+C\nu^{-1}\delta^2\|\nabla\mathbf{u}_h^{n+1/2}\|^2. \qquad (4.5)
\end{aligned}$$

Now,

$$\begin{aligned}
&\frac{1}{2\Delta t}\big(\|\mathbf{s}_h^{n+1}\|^2-\|\mathbf{s}_h^{n}\|^2\big)+\frac{\nu}{2}\|\nabla\mathbf{s}_h^{n+1/2}\|^2\\
\le&C\nu^3\big(\|\nabla(\mathbf{u}^{n+1/2}-\mathbf{u}_h^{n+1/2})\|^4+\|\nabla\mathbf{u}^{n+1/2}\|^4\big)\|\mathbf{s}_h^{n+1/2}\|^2+C\nu^{-1}\delta^2\|\nabla\mathbf{u}_h^{n+1/2}\|^2.
\end{aligned}$$

Summing up from $l=1,\cdots n$, and multiplying by $2\Delta t$

$$\begin{aligned}
&\|\mathbf{s}_h^{n+1}\|^2+\nu\Delta t\sum_{l=0}^{n}\|\nabla\mathbf{s}_h^{n+1/2}\|^2\\
\le&C\nu^3\Delta t\sum_{l=0}^{n}\big(\|\nabla(\mathbf{u}^{n+1/2}-\mathbf{u}_h^{n+1/2})\|^4+\|\nabla\mathbf{u}^{n+1/2}\|^4\big)\|\mathbf{s}_h^{n+1/2}\|^2\\
&+\|\mathbf{s}_h^0\|^2+C\nu^{-1}\delta^2\Delta t\sum_{l=0}^{n}\|\nabla\mathbf{u}_h^{n+1/2}\|^2.
\end{aligned}$$

Note that $\|\mathbf{s}_h^0\|=0$, and the last term in the above estimate is bounded by the previous Lemma 4.1. After applying the Gronwall's lemma, we obtain the result

$$\|\mathbf{s}_h^{n+1}\|^2+\nu\Delta t\sum_{l=0}^{n}\|\nabla\mathbf{s}_h^{n+1/2}\|^2\le C\nu^{-2}\delta^2\Big(\Delta t\sum_{l=0}^{n}\|\nabla\mathbf{f}^{n+1/2}\|^2+\|\mathbf{u}_h^0\|^2\Big).$$

Given $\mathbf{s}_h^n$, the problem of finding $\mathbf{s}_h^{n+1}$ satisfying (3.6a)-(3.6b) is linear and finite-dimensional. Therefor, it suffices to show uniqueness of the solution, and this is easily obtained based on the derived stability bound, by letting the problem data equal to zero on the RHS. □

4.2 Error estimates

Herein, we prove the convergence of the approximated finite element sensitivity solution to (1.4), using the numerical scheme given by (3.4a)-(3.4c).

First we present a lemma that will be applied in the main error estimate in Theorem 4.1. This lemma gives the finite element error estimate for the sensitivity filter problem given by (1.5).

Lemma 4.3. *Let* $(\mathbf{s},r)$ *be a smooth, strong sensitivity solution satisfying* (1.4)*, and* $(\mathbf{s}_h,r_h)$ *be the finite element sensitivity solution satisfying* (3.4a)-(3.4c)*, and let* $\mathbf{w}$ *be a smooth, strong sensitivity solution satisfying* (1.5)*, and* $\mathbf{w}_h$ *be the finite element sensitivity solution satisfying* (3.4c)*. Then, the following estimate holds at the given time step n*

$$\|\mathbf{w}^{n+1/2}-\mathbf{w}_h^{n+1/2}\|^2 \le C\delta^2 h^{2k}|\mathbf{s}|_{k+1}^2 + Ch^{2k+2}|\mathbf{s}|_{k+1}^2 + \|\mathbf{s}^{n+1/2}-\mathbf{s}_h^{n+1/2}\|^2.$$

Proof. To find a bound for $\|\mathbf{w}^{n+1/2}-\mathbf{w}_h^{n+1/2}\|$, we start by subtracting (3.4c) from (3.2c) evaluated at t^{n+1} to get

$$\delta^2(\nabla\mathbf{w}^{n+1}-\nabla\mathbf{w}_h^{n+1},\nabla v_h)+(\mathbf{w}^{n+1}-\mathbf{w}_h^{n+1},\mathbf{v}_h)=(\mathbf{s}^{n+1}-\mathbf{s}_h^{n+1},\mathbf{v}_h), \quad \forall \mathbf{v}_h\in X^h.$$

Averaging out the above equation, we get

$$\delta^2(\nabla\mathbf{w}^{n+1/2}-\nabla\mathbf{w}_h^{n+1/2},\nabla v_h)+(\mathbf{w}^{n+1/2}-\mathbf{w}_h^{n+1/2},\mathbf{v}_h)=(\mathbf{s}^{n+1/2}-\mathbf{s}_h^{n+1/2},\mathbf{v}_h), \quad \forall \mathbf{v}_h\in X^h.$$

Let $\mathbf{E}^{n+1}=\mathbf{w}^{n+1}-\mathbf{w}_h^{n+1}=(\mathbf{w}^{n+1}-\mathbf{W}^{n+1})-(\mathbf{w}_h^{n+1}-\mathbf{W}^{n+1})=\boldsymbol{\theta}^{n+1}-\boldsymbol{\varphi}_h^{n+1}$, with $\mathbf{W}\in X^h$, and also pick $\mathbf{v}=\boldsymbol{\varphi}_h^{n+1/2}$. Then,

$$\begin{aligned}
&\delta^2\|\nabla\boldsymbol{\varphi}_h^{n+1/2}\|^2+\|\boldsymbol{\varphi}_h^{n+1/2}\|^2\\
=&\delta^2(\nabla\boldsymbol{\theta}^{n+1/2},\nabla\boldsymbol{\varphi}_h^{n+1/2})+(\boldsymbol{\theta}^{n+1/2},\boldsymbol{\varphi}_h^{n+1/2})-(\mathbf{s}^{n+1/2}-\mathbf{s}_h^{n+1/2},\boldsymbol{\varphi}_h^{n+1/2})\\
\le&\frac{\delta^2}{2}\|\nabla\boldsymbol{\varphi}_h^{n+1/2}\|+\frac{\delta^2}{2}\|\nabla\boldsymbol{\theta}^{n+1/2}\|^2+\frac{1}{2}\|\boldsymbol{\varphi}_h^{n+1/2}\|^2+\|\boldsymbol{\theta}^{n+1/2}\|^2+\|\mathbf{s}^{n+1/2}-\mathbf{s}_h^{n+1/2}\|^2.
\end{aligned}$$

Thus

$$\frac{\delta^2}{2}\|\nabla\boldsymbol{\varphi}_h^{n+1/2}\|^2+\frac{1}{2}\|\boldsymbol{\varphi}_h^{n+1/2}\|^2\le\frac{\delta^2}{2}\|\nabla\boldsymbol{\theta}^{n+1/2}\|^2+\|\boldsymbol{\theta}^{n+1/2}\|^2+\|\mathbf{s}^{n+1/2}-\mathbf{s}_h^{n+1/2}\|^2.$$

Dropping the first term from the LHS of the above equation and multiplying by 2,

$$\|\boldsymbol{\varphi}_h^{n+1/2}\|^2\le C\delta^2\|\nabla\boldsymbol{\theta}^{n+1/2}\|^2+C\|\boldsymbol{\theta}^{n+1/2}\|^2+C\|\mathbf{s}^{n+1/2}-\mathbf{s}_h^{n+1/2}\|^2.$$

Triangle inequality (i.e., $\|\mathbf{w}-\mathbf{w}_h\|\le\|\boldsymbol{\theta}\|+\|\boldsymbol{\varphi}_h\|$) yields

$$\begin{aligned}
\|\mathbf{w}^{n+1/2}-\mathbf{w}_h^{n+1/2}\|^2 &\le C\delta^2\|\nabla\boldsymbol{\theta}^{n+1/2}\|^2+C\|\boldsymbol{\theta}^{n+1/2}\|^2+C\|\mathbf{s}^{n+1/2}-\mathbf{s}_h^{n+1/2}\|^2\\
&\le C\delta^2h^{2k}|\mathbf{w}|_{k+1}^2+Ch^{2k+2}|\mathbf{w}|_{k+1}^2+\|\mathbf{s}^{n+1/2}-\mathbf{s}_h^{n+1/2}\|^2\\
&\le C\delta^2h^{2k}|\mathbf{s}|_{k+1}^2+Ch^{2k+2}|\mathbf{s}|_{k+1}^2+\|\mathbf{s}^{n+1/2}-\mathbf{s}_h^{n+1/2}\|^2. \qquad (4.6)
\end{aligned}$$

Thus, we complete the proof. ☐

Next, we present the sensitivity error estimates.

Theorem 4.1. *Let* $(\mathbf{s},r)$ *be a smooth, strong sensitivity solution satisfying* (1.4), *and* $(\mathbf{s}_h,r_h)$ *be the finite element sensitivity solution satisfying* (3.4a)-(3.4c), *on the interval* $[0,T]$ *such that* $\nabla(\mathbf{u}-\mathbf{u}_h)\in l^4(L_2)$. *Then, for* Δt *small enough (and the restriction is precisely stated in the proof of the theorem), we have the following*

$$\|s-s_h\|_{\infty,0}^2+\nu\Delta t\sum_{n=0}^{N}\|\nabla(s^{n+1/2}-s_h^{n+1/2})\|^2\leq Ch^{2k}\||s|\|_{\infty,0}^2+F(\Delta t,h,\delta,\chi)$$

with

$$\begin{aligned}F(\Delta t,h,\delta,\chi)=&C\big\{(\nu+\nu^{-1}+\nu^{-1}\chi^2\delta^2)h^{2k}\||\mathbf{s}|\|_{2,k+1}^2+(\chi+\nu^{-1}\chi^2)h^{2k+2}\||\mathbf{s}|\|_{2,k+1}^2\\&+\nu^{-1}h^{2s+2}\||r|\|_{2,s+1}^2+C(\mathbf{u}_0,\mathbf{u},\mathbf{f})(h^{2k}+h^{2s+2}+\Delta t^4)+C(\mathbf{u}_0,\mathbf{f})\nu^{-2}h^{2k}\\&+C\nu^{-1}h^{2k}(\||\nabla\mathbf{u}|\|_{4,0}^4+\||\nabla(\mathbf{u}-\mathbf{u}_h)|\|_{4,0}^4+\||\mathbf{s}|\|_{4,k+1}^4)\big\}.\end{aligned}$$

Proof. At time $t^{n+1/2}=(t^{n+1}+t^n)/2$, (3.2a) may be written as

$$\begin{aligned}&\frac{1}{\Delta t}(\mathbf{s}^{n+1}-\mathbf{s}^n,\mathbf{v})+\nu a(\mathbf{s}^{n+1/2},\mathbf{v})+b^*(\mathbf{s}^{n+1/2},\mathbf{u}^{n+1/2},\mathbf{v})+b^*(\mathbf{u}^{n+1/2},\mathbf{s}^{n+1/2},\mathbf{v})\\&\quad-(r^{n+1/2},\nabla\cdot\mathbf{v})+(\mathbf{u}^{n+1/2}-\overline{\mathbf{u}}^{h^{n+1/2}},\mathbf{v})+\chi(\mathbf{s}^{n+1/2}-\mathbf{w}^{n+1/2},\mathbf{v})\\&=Int(\mathbf{s}^{n+1},r^{n+1};\mathbf{v}),\quad\forall\mathbf{v}\in V^h,\end{aligned}\tag{4.7}$$

where

$$\begin{aligned}&Int(\mathbf{s}^{n+1},r^{n+1};\mathbf{v})\\&=\Big(\frac{\mathbf{s}^{n+1}-\mathbf{s}^n}{\Delta t}-\mathbf{s}_t,\mathbf{v}\Big)+\nu a(\mathbf{s}^{n+1/2}-\mathbf{s}(t^{n+1/2}),\mathbf{v})+b^*(\mathbf{s}^{n+1/2},\mathbf{u}^{n+1/2},\mathbf{v})\\&\quad-b^*(\mathbf{s}(t^{n+1/2}),\mathbf{u}(t^{n+1/2}),\mathbf{v})+b^*(\mathbf{u}^{n+1/2},\mathbf{s}^{n+1/2},\mathbf{v})-b^*(\mathbf{u}(t^{n+1/2}),\mathbf{s}(t^{n+1/2}),\mathbf{v})\\&\quad-(r^{n+1/2}-r(t^{n+1/2}),\nabla\cdot\mathbf{v})+(\mathbf{u}^{n+1/2}-\overline{\mathbf{u}}^{h^{n+1/2}},\mathbf{v})-(\mathbf{u}(t^{n+1/2})-\overline{\mathbf{u}}(t^{n+1/2}),\mathbf{v})\\&\quad+\chi(\mathbf{s}^{n+1/2}-\mathbf{w}^{n+1/2},\mathbf{v})-\chi(\mathbf{s}(t^{n+1/2})-\mathbf{w}(t^{n+1/2}),\mathbf{v}),\end{aligned}$$

is the interpolation and filtering error. Subtracting (3.6a) from (4.7), we have for $\mathbf{e}^{n+1}=\mathbf{s}^{n+1}-\mathbf{s}_h^{n+1}$ and $\boldsymbol{\varepsilon}^{n+1}=\mathbf{u}^{n+1}-\mathbf{u}_h^{n+1}$,

$$\begin{aligned}&\frac{1}{\Delta t}(\mathbf{e}^{n+1}-\mathbf{e}^n,\mathbf{v})+\nu a(\mathbf{e}^{n+1/2},\mathbf{v})+b^*(\mathbf{s}^{n+1/2},\mathbf{u}^{n+1/2},\mathbf{v})+b^*(\mathbf{u}^{n+1/2},\mathbf{s}^{n+1/2},\mathbf{v})\\&-b^*(\mathbf{s}_h^{n+1/2},\mathbf{u}_h^{n+1/2},\mathbf{v})-b^*(\mathbf{u}_h^{n+1/2},\mathbf{s}_h^{n+1/2},\mathbf{v})-(r^{n+1/2},\nabla\cdot\mathbf{v})+(\boldsymbol{\varepsilon}^{n+1/2}-\overline{\boldsymbol{\varepsilon}}^{n+1/2},\mathbf{v})\\&+\chi(\mathbf{e}^{n+1/2},\mathbf{v})-\chi(\mathbf{w}^{n+1/2}-\mathbf{w}_h^{n+1/2},\mathbf{v})=Int(\mathbf{s}^{n+1},r^{n+1};\mathbf{v}),\quad\forall\mathbf{v}\in V^h.\end{aligned}\tag{4.8}$$

Set $\mathbf{e}^{n+1}=\mathbf{s}^{n+1}-\tilde{\mathbf{s}}^{n+1}-(\mathbf{s}_h^{n+1}-\tilde{\mathbf{s}}^{n+1})=\boldsymbol{\eta}^{n+1}-\boldsymbol{\phi}_h^{n+1}$, with $\tilde{\mathbf{s}}\in V_h$. Based on Eq. (4.8), with the choice $\mathbf{v}=\boldsymbol{\phi}_h^{n+1/2}$, and using that $(q,\nabla\cdot\boldsymbol{\phi}_h^{n+1/2})=0$, $\forall q\in Q_h$, we obtain

$$\begin{aligned}
&\frac{1}{2\Delta t}(\|\boldsymbol{\phi}_h^{n+1}\|^2-\|\boldsymbol{\phi}_h^{n}\|^2)+\nu\|\nabla\boldsymbol{\phi}_h^{n+1/2}\|^2+\chi\|\boldsymbol{\phi}_h^{n+1/2}\|^2\\
=&\frac{1}{\Delta t}(\boldsymbol{\eta}^{n+1}-\boldsymbol{\eta}^{n},\boldsymbol{\phi}_h^{n+1/2})+\nu a(\boldsymbol{\eta}^{n+1/2},\boldsymbol{\phi}_h^{n+1/2})+b^*(\mathbf{s}^{n+1/2},\mathbf{u}^{n+1/2},\boldsymbol{\phi}_h^{n+1/2})\\
&+b^*(\mathbf{u}^{n+1/2},\mathbf{s}^{n+1/2},\boldsymbol{\phi}_h^{n+1/2})-b^*(\mathbf{s}_h^{n+1/2},\mathbf{u}_h^{n+1/2},\boldsymbol{\phi}_h^{n+1/2})-b^*(\mathbf{u}_h^{n+1/2},\mathbf{s}_h^{n+1/2},\boldsymbol{\phi}_h^{n+1/2})\\
&-(r^{n+1/2}-q,\nabla\cdot\boldsymbol{\phi}_h^{n+1/2})+(\varepsilon^{n+1/2}-\overline{\varepsilon}^{n+1/2},\boldsymbol{\phi}_h^{n+1/2})+\chi(\boldsymbol{\eta}^{n+1/2},\boldsymbol{\phi}_h^{n+1/2})\\
&-\chi(\mathbf{w}^{n+1/2}-\mathbf{w}_h^{n+1/2},\boldsymbol{\phi}_h^{n+1/2})-Int(\mathbf{s}^{n+1},r^{n+1};\boldsymbol{\phi}_h^{n+1/2}),\quad \forall\mathbf{v}\in V^h. \qquad (4.9)
\end{aligned}$$

By choosing $\tilde{\mathbf{s}}$ to be the L^2 projection of $\mathbf{s}$ in V_h, we have that the first term vanishes,

$$(\boldsymbol{\eta}^{n+1}-\boldsymbol{\eta}^{n},\boldsymbol{\phi}_h^{n+1/2})=0. \qquad (4.10)$$

Next, we rewrite the nonlinear terms $b^*(\cdot,\cdot,\cdot)$ as following

$$\begin{aligned}
&b^*(\mathbf{s}^{n+1/2},\mathbf{u}^{n+1/2},\boldsymbol{\phi}_h^{n+1/2})+b^*(\mathbf{u}^{n+1/2},\mathbf{s}^{n+1/2},\boldsymbol{\phi}_h^{n+1/2})\\
&-b^*(\mathbf{s}_h^{n+1/2},\mathbf{u}_h^{n+1/2},\boldsymbol{\phi}_h^{n+1/2})-b^*(\mathbf{u}_h^{n+1/2},\mathbf{s}_h^{n+1/2},\boldsymbol{\phi}_h^{n+1/2})\\
=&b^*(\boldsymbol{\eta}^{n+1/2},\mathbf{u}^{n+1/2},\boldsymbol{\phi}_h^{n+1/2})-b^*(\boldsymbol{\phi}_h^{n+1/2},\mathbf{u}^{n+1/2},\boldsymbol{\phi}_h^{n+1/2})+b^*(\mathbf{u}^{n+1/2},\mathbf{s}^{n+1/2},\boldsymbol{\phi}_h^{n+1/2})\\
&+b^*(\mathbf{s}_h^{n+1/2},\mathbf{u}^{n+1/2}-\mathbf{u}_h^{n+1/2},\boldsymbol{\phi}_h^{n+1/2})-b^*(\mathbf{u}_h^{n+1/2},\mathbf{s}_h^{n+1/2},\boldsymbol{\phi}_h^{n+1/2})\\
=&b^*(\boldsymbol{\eta}^{n+1/2},\mathbf{u}^{n+1/2},\boldsymbol{\phi}_h^{n+1/2})-b^*(\boldsymbol{\phi}_h^{n+1/2},\mathbf{u}^{n+1/2},\boldsymbol{\phi}_h^{n+1/2})\\
&+b^*(\mathbf{s}_h^{n+1/2},\mathbf{u}^{n+1/2}-\mathbf{u}_h^{n+1/2},\boldsymbol{\phi}_h^{n+1/2})+b^*(\mathbf{u}_h^{n+1/2},\boldsymbol{\eta}^{n+1/2},\boldsymbol{\phi}_h^{n+1/2})\\
&-b^*(\mathbf{u}_h^{n+1/2},\boldsymbol{\phi}_h^{n+1/2},\boldsymbol{\phi}_h^{n+1/2})+b^*(\mathbf{u}^{n+1/2}-\mathbf{u}_h^{n+1/2},\mathbf{s}^{n+1/2},\boldsymbol{\phi}_h^{n+1/2}).
\end{aligned}$$

Now, we bound each term from the RHS of Eq. (4.9) including the expanded nonlinear terms as above. We apply Cauchy-Schwarz and then Young's inequality to each term (see the bounds in Appendix). Inserting all the bounds into (4.9) and using the bound on $\|\mathbf{w}^{n+1/2}-\mathbf{w}_h^{n+1/2}\|^2$ from the Lemma 4.3, one obtains

$$\begin{aligned}
&\frac{1}{2\Delta t}(\|\boldsymbol{\phi}_h^{n+1}\|^2-\|\boldsymbol{\phi}_h^{n}\|^2)+\frac{\nu}{2}\|\nabla\boldsymbol{\phi}_h^{n+1/2}\|^2+\frac{\chi}{2}\|\boldsymbol{\phi}_h^{n+1/2}\|^2\\
\le&C\nu\|\nabla\boldsymbol{\eta}^{n+1/2}\|^2+C\nu^{-1}\|r^{n+1/2}-q\|^2+C\nu^{-1}\|\nabla(\mathbf{u}^{n+1/2}-\mathbf{u}_h^{n+1/2})\|^2+C\chi\|\boldsymbol{\eta}^{n+1/2}\|^2\\
&+C\nu^{-1}\chi^2\|\mathbf{w}^{n+1/2}-\mathbf{w}_h^{n+1/2}\|^2+C\nu^{-1}\|\nabla\mathbf{u}^{n+1/2}\|^2\|\nabla\boldsymbol{\eta}^{n+1/2}\|^2\\
&+C\nu^{-3}\|\nabla\mathbf{u}^{n+1/2}\|^4\|\boldsymbol{\phi}_h^{n+1/2}\|^2+C\nu^{-1}\|\boldsymbol{\eta}^{n+1/2}\|\|\nabla\boldsymbol{\eta}^{n+1/2}\|\|\nabla(\mathbf{u}^{n+1/2}-\mathbf{u}_h^{n+1/2})\|^2\\
&+C\nu^{-1}\|\nabla\mathbf{u}_h^{n+1/2}\|\|\nabla\boldsymbol{\eta}^{n+1/2}\|^2+C\nu^{-1}\|\nabla(\mathbf{u}^{n+1/2}-\mathbf{u}_h^{n+1/2})\|^2\|\nabla\mathbf{s}^{n+1/2}\|^2\\
&+|Int(\mathbf{s}^{n+1},r^{n+1};\boldsymbol{\phi}_h^{n+1/2})|+C\nu^{-3}\|\nabla(\mathbf{u}^{n+1/2}-\mathbf{u}_h^{n+1/2})\|^4\|\boldsymbol{\phi}_h^{n+1/2}\|^2.
\end{aligned}$$

Summing from $n=0$ to N, multiplying by $2\Delta t$, and assuming $\|\boldsymbol{\phi}_h^0\|=0$, we have

$$\begin{aligned}
&\|\boldsymbol{\phi}_h^{N+1}\|^2+\nu\Delta t\sum_{n=0}^{N}\|\nabla\boldsymbol{\phi}_h^{n+1/2}\|^2+\chi\Delta t\sum_{n=0}^{N}\|\boldsymbol{\phi}_h^{n+1/2}\|^2\\
\le&\Delta t\sum_{n=0}^{N}C\nu^{-3}(\|\nabla\mathbf{u}^{n+1/2}\|^4+\|\nabla(\mathbf{u}^{n+1/2}-\mathbf{u}_h^{n+1/2})\|^4)\|\boldsymbol{\phi}_h^{n+1/2}\|^2+\Delta t\sum_{n=0}^{N}C\nu\|\nabla\boldsymbol{\eta}^{n+1/2}\|^2\\
&+\Delta t\sum_{n=0}^{N}C\chi\|\boldsymbol{\eta}^{n+1/2}\|^2+\Delta t\sum_{n=0}^{N}C\nu^{-1}\|r^{n+1/2}-q\|^2+\Delta t\sum_{n=0}^{N}C\nu^{-1}\|\nabla(\mathbf{u}^{n+1/2}-\mathbf{u}_h^{n+1/2})\|^2\\
&+\Delta t\sum_{n=0}^{N}C\nu^{-1}\chi^2\|\mathbf{w}^{n+1/2}-\mathbf{w}_h^{n+1/2}\|^2+\Delta t\sum_{n=0}^{N}C\nu^{-1}\|\nabla\mathbf{u}^{n+1/2}\|^2\|\nabla\boldsymbol{\eta}^{n+1/2}\|^2\\
&+\Delta t\sum_{n=0}^{N}C\nu^{-1}\|\boldsymbol{\eta}^{n+1/2}\|\|\nabla\boldsymbol{\eta}^{n+1/2}\|\|\nabla(\mathbf{u}^{n+1/2}-\mathbf{u}_h^{n+1/2})\|^2\\
&+\Delta t\sum_{n=0}^{N}C\nu^{-1}\|\nabla\mathbf{u}_h^{n+1/2}\|\|\nabla\boldsymbol{\eta}^{n+1/2}\|^2+\Delta t\sum_{n=0}^{N}C\nu^{-1}\|\nabla(\mathbf{u}^{n+1/2}-\mathbf{u}_h^{n+1/2})\|^2\|\nabla\mathbf{s}^{n+1/2}\|^2\\
&+\Delta t\sum_{n=0}^{N}|Int(\mathbf{s}^{n+1},r^{n+1};\boldsymbol{\phi}_h^{n+1/2})|. \qquad (4.11)
\end{aligned}$$

Technically, we want to bound the RHS of (4.11). This is done applying Eqs. (2.1a)-(2.1c) (see the Appendix). Combining all the bounds shown in Appendix, we get

$$\begin{aligned}
&\|\boldsymbol{\phi}_h^{N+1}\|^2+\nu\Delta t\sum_{n=0}^{N}\|\nabla\boldsymbol{\phi}_h^{n+1/2}\|^2+\chi\Delta t\sum_{n=0}^{N}\|\boldsymbol{\phi}_h^{n+1/2}\|^2\\
\le&\Delta t\sum_{n=0}^{N}C(1+\nu^{-1}\chi^2+\nu^{-3}\|\nabla\mathbf{u}^{n+1/2}\|^4+\|\nabla(\mathbf{u}^{n+1/2}-\mathbf{u}_h^{n+1/2})\|^4)\|\boldsymbol{\phi}_h^{n+1}\|^2\\
&+C\nu h^{2k}|||\mathbf{s}|||^2_{2,k+1}+C\chi h^{2k+2}|||\mathbf{s}|||^2_{2,k+1}+C\nu^{-1}h^{2s+2}|||r|||^2_{2,s+1}\\
&+C(\mathbf{u}_0,\mathbf{u},\mathbf{f})\nu^{-2}(h^{2k}+h^{2s+2}+\Delta t^4)+C\nu^{-1}\chi^2\delta^2h^{2k}|||\mathbf{s}|||^2_{2,k+1}+C\nu^{-1}\chi^2h^{2k+2}|||\mathbf{s}|||^2_{2,k+1}\\
&+C\nu^{-1}h^{2k}(|||\nabla\mathbf{u}|||^4_{4,0}+|||\mathbf{s}|||^4_{4,k+1})+C\nu^{-1}h^{2k}|||\nabla(\mathbf{u}-\mathbf{u}_h)|||^4_{4,0}\\
&+C(\mathbf{u}_0,\mathbf{f})\nu^{-2}h^{2k}+C\nu^{-1}h^{2k}|||\mathbf{s}|||^2_{2,k+1}.
\end{aligned}$$

Hence, with Δt sufficiently small, i.e.,

$$\Delta t<C(1+\nu^{-1}\chi^2+\nu^{-3}\|\nabla\mathbf{u}^{n+1/2}\|^4_{4,0}+|||\nabla(\mathbf{u}-\mathbf{u}_h)|||^4_{4,0})^{-1}$$

from Gronwall's Lemma, we have

$$\begin{aligned}
&\|\boldsymbol{\phi}_h^{N+1}\|^2+\nu\Delta t\sum_{n=0}^{N}\|\nabla\boldsymbol{\phi}_h^{n+1/2}\|^2+\chi\Delta t\sum_{n=0}^{N}\|\boldsymbol{\phi}_h^{n+1/2}\|^2\\
\le&C\big\{(\nu+\nu^{-1}+\nu^{-1}\chi^2\delta^2)h^{2k}|||\mathbf{s}|||^2_{2,k+1}+(\chi+\nu^{-1}\chi^2)h^{2k+2}|||\mathbf{s}|||^2_{2,k+1}
\end{aligned}$$

$$+\nu^{-1}h^{2s+2}|||r|||^2_{2,s+1}+C(\mathbf{u}_0,\mathbf{u},\mathbf{f})(h^{2k}+h^{2s+2}+\Delta t^4)+C(\mathbf{u}_0,\mathbf{f})\nu^{-2}h^{2k}$$
$$+C\nu^{-1}h^{2k}(|||\nabla\mathbf{u}|||^4_{4,0}+|||\nabla(\mathbf{u}-\mathbf{u}_h)|||^4_{4,0}+|||\mathbf{s}|||^4_{4,k+1})\}.$$

Using triangle inequality we obtain the stated estimate of the theorem. □

Remark 4.1. The above theorem shows the convergence of the finite element solution of sensitivity of TRM towards the true sensitivity of the TRM given by (3.2a)-(3.2c), as h and Δt tend to 0, i.e.,

$$\|s-s_h\|^2_{\infty,0}+\nu\Delta t\sum_{n=0}^{N}\|\nabla(s^{n+1/2}-s_h^{n+1/2})\|^2=\mathcal{O}(h^{2k}+h^{2s+2}+\Delta t^4).$$

This estimate is optimal in space and time since the second order Crank-Nicolson scheme is applied for time discretization.

5 Sensitivity computations

The goal of this section is first to provide a numerical study illustrating the convergence results for the fully discrete sensitivity equation in (3.6a) and (3.6b) and to show a comparison of the sensitivity computations via two different approaches, one using the discretized sensitivity equations (3.6a) and (3.6b) and the other using the forward finite difference given by (1.3). All calculations presented in this paper were obtained using the publicly available finite element software package FreeFEM++, see [26]. In these studies, we have used the 2D Taylor-Green vortex decay problem and the 2D Cavity problem as our test problems, see [38,39] (for sensitivity computations of two different fluid models with respect to the filter width using 2D Cavity problem). In addition, we examine the sensitivity computations in a three dimensional case study using the 3D Ethier-Steinman benchmark problem, see [16,38] for flow velocity and its sensitivity computations based on the variations of filter width δ. All the presented computations in this section, study the the sensitivity of the TRM with respect to the time relaxation coefficient χ given filter width $\delta=h$.

5.1 Convergence study

Convergence results for the numerical scheme in (3.6a) and (3.6b) using a mesh refinement are given in this section. The numerical experiment is performed on the 2D Taylor-Green vortex decay problem with a solution consisting of an $n\times n$ array of oppositely signed vortices decaying as $t\rightarrow 0$. The test problem used in this experiment was defined and studied in [14,18,43]. The problem is defined on the unit square and it is known to have the following true solution of the Navier-Stokes equations given $\tau = Re$ and $f = 0$,

$$\mathbf{u}_1 = -\cos(n\pi x)\sin(n\pi y)\exp(-2n^2\pi^2 t/\tau), \tag{5.1a}$$

$$\mathbf{u}_2 = \sin(n\pi x)\cos(n\pi y)\exp(-2n^2\pi^2 t/\tau), \tag{5.1b}$$

$$\mathbf{p} = -\frac{1}{4}(\cos(2n\pi x)+\cos(2n\pi y))\exp(-4n^2\pi^2 t/\tau). \tag{5.1c}$$

The sensitivity s_h is computed at each time-step t^n using the scheme in (3.6a) and (3.6b) through computing $\mathbf{u}(t^n)$ and $\mathbf{u}(t^{n+1})$ from (5.1b) and using them in Eq. (3.5b) to obtain corresponding $\overline{\mathbf{u}}$ values. We use the approximation solution with a mesh size $h^* = 1/100$ as the sensitivity true solution of (3.6a). For the error computations, a sequence of grids is generated with the structure $h_k = 1/20k$, for $k = 1,2,3,4$. These computations are obtained using the following parameters: uniform time step $\Delta t = 0.001$, final time $T = 0.1$, time relaxation parameter $\chi = 0.01$, order of deconvolution $N = 0$, $n = 1$, and $\tau = Re$ with different values of $Re = 1,5,10$. Given a grid size, denoted by h, the sensitivity error calculation is defined as follows

$$E(h) = \|s_{h^*} - s_h\|_{l^2(0,T;L^2(\Omega))}, \quad \text{where} \quad \|u\|_{l^2(0,T;L^2(\Omega)} = \Big[\Delta t \sum_{i=0}^{N} \|u(i\Delta t)\|^q_{L^p}\Big]^{1/q}.$$

Figs. 1 and 2 show the error computations of $E(h)$ using Taylor-Hood $P2/P1$ and mini elements $Pb1/P1$ along with their log-log plot. According to the data presented by these figures, $E(h)$ decreases with the mesh refinement for all tested Re values, but its value is larger for larger Reynolds number.

The experimental convergence rates presented in Tables 1 and 2 are determined by calculating the errors at two successive values of h by postulating $E(h) = Ch^a$ and solving for exponent a in expression $(h_1/h_2)^a = E(h_1)/E(h_2)$. The results of the following tables

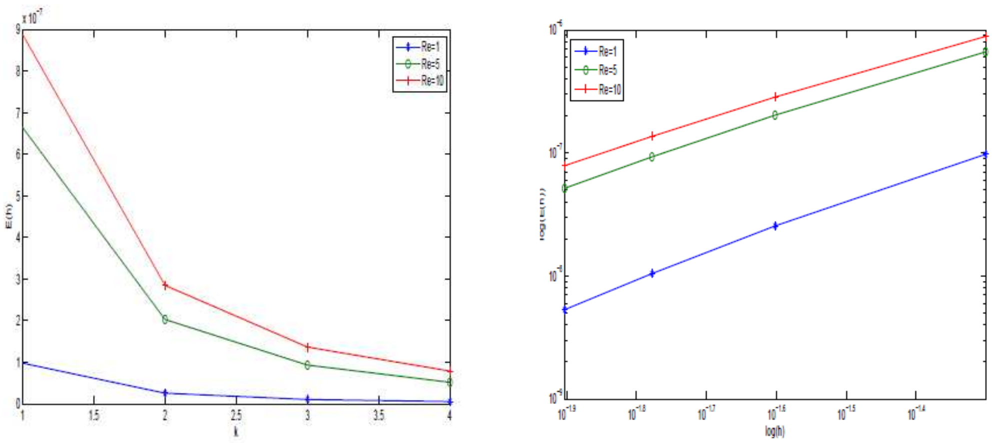

(a) (b)

Figure 1: Sensitivity error and its log-log plot (from (a) to (b)) using P2/P1 finite elements.

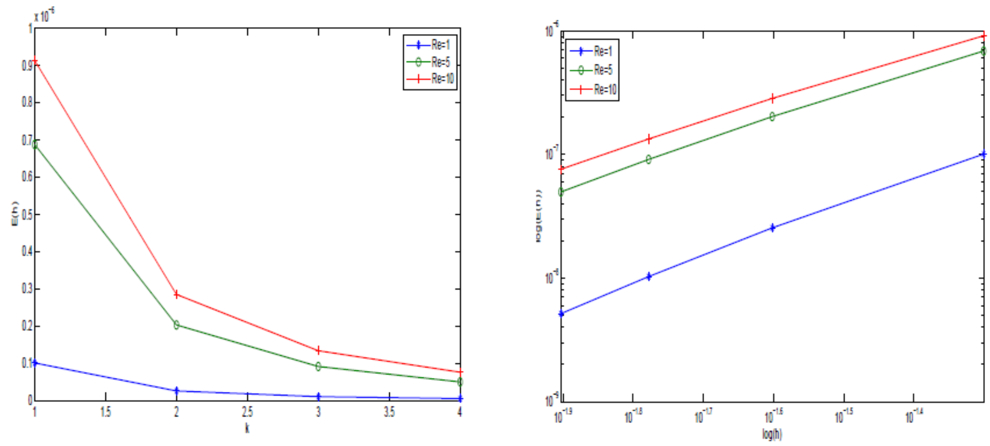

(a) (b)

Figure 2: Sensitivity error and its log-log plot (from (a) to (b)) using Pb1/P1 finite elements.

and the log-log plots show that the convergence rates agree with the theoretical results stated in Theorem 4.1. With our choice of spaces, we expect a rate of convergence 2 for all selected Re values.

Table 1: Velocity errors and rate of convergence for different values of Re using P2/P1 finite elements.

	$Re=1$		$Re=5$		$Re=10$	
h	$E(h)$	rate	$E(h)$	rate	$E(h)$	rate
$\frac{1}{20}$	9.76609e-008		6.64465e-007		8.88055e-007	
$\frac{1}{40}$	2.54884e-008	1.9379	2.02893e-007	1.7115	2.85052e-007	1.6394
$\frac{1}{60}$	1.04382e-008	2.2018	9.29938e-008	1.9241	1.3634e-007	1.8189
$\frac{1}{80}$	5.31311e-009	2.3474	5.16102e-008	2.0468	7.87598e-008	1.9075

Table 2: Velocity errors and rate of convergence for different values of Re using Pb1/P1 finite elements.

	$Re=1$		$Re=5$		$Re=10$	
h	$E(h)$	rate	$E(h)$	rate	$E(h)$	rate
$\frac{1}{20}$	1.00669e-007		6.86467e-007		9.11968e-007	
$\frac{1}{40}$	2.54847e-008	1.9819	2.02754e-007	1.7595	2.8445e-007	1.6808
$\frac{1}{60}$	1.02827e-008	2.2385	9.11979e-008	1.9705	1.33442e-007	1.8667
$\frac{1}{80}$	5.15958e-009	2.3971	4.98027e-008	2.1029	7.59743e-008	1.9580

5.2 2D Cavity Problem

In this section, we present our results in sensitivity computations via two different strategies, SEM and FFD. The numerical experiments are performed on the 2D Cavity problem. The flow domain Ω is $[0,1]\times[0,1]$. The upper boundary moves with the velocity

Table 3: Sensitivity computations using SEM and FFD for $Re=1000$.

χ	Method	$t=0.1$	$t=1$
0.01	SEM	0.00356199	0.0157713
	FFD	0.0035127	0.0161915
0.1	SEM	0.00353882	0.0151647
	FFD	0.00349686	0.015834
1	SEM	0.00331772	0.0110461
	FFD	0.00334363	0.0128588
10	SEM	0.00193639	0.00747537
	FFD	0.00222443	0.00373012

Table 4: Sensitivity computations using SEM and FFD for $Re=5000$.

χ	Method	$t=0.1$	$t=1$
0.01	SEM	0.00464835	0.0302347
	FFD	0.00455709	0.0331724
0.1	SEM	0.00461516	0.0287494
	FFD	0.00453252	0.0318776
1	SEM	0.00429915	0.0188134
	FFD	0.00429606	0.0222439
10	SEM	0.00235258	0.00878799
	FFD	0.002640837	0.00424233

Table 5: Sensitivity computations using SEM and FFD for $Re=10000$.

χ	Method	$t=0.1$	$t=1$
0.01	SEM	0.00491548	0.0363773
	FFD	0.00481204	0.0415477
0.1	SEM	0.00487968	0.0344382
	FFD	0.00478515	0.039622
1	SEM	0.00453911	0.02162
	FFD	0.00452661	0.0258911
10	SEM	0.00244766	0.0090533
	FFD	0.00273327	0.0043209

$\mathbf{u}=(16x^2(1-x)^2,0)^t$ and there is a zero boundary condition else where. The initial data is chosen to be $\mathbf{u}(0,x,y)=(3y^2-2y,0)^t$ in Ω. Since the initial and boundary conditions for $\mathbf{u}$ do not depend on χ, we have zero initial and boundary conditions for the sensitivity $\mathbf{s}$.

All the computations are carried out with a uniform time step $\Delta t=0.01$ using the Taylor-Hood finite elements. Let s_{SEM} and s_{FFD} denote the sensitivity computations using SEM and FFD, respectively. Tables 3-5 represent $\|s_{SEM}\|_{L^2(\Omega)}$ and $\|s_{FFD}\|_{L^2(\Omega)}$ for Reynolds numbers 1000, 5000, and 10000, for different values of time relaxation parameter $\chi=0.01,0.1,1$, and 10, with $\Delta\chi=0.001$ at times $t=0.1$, and 1. These computations are done using a fixed spatial mesh size of $h=1/36$.

For all tested Re values, one observes the following,

- A larger scale of sensitivity is obtained as time has progressed to $t=1$ via both approaches for all chosen χ values.
- A decrease in sensitivity values is observed as χ values increase from 0.01 to 10 at both times, i.e., $t=0.1$, and 1.
- Larger Raeynolds numbers show larger sensitivities especially at $t=1$.
- $\|s_{SEM}\|_{L^2(\Omega)}$ and $\|s_{FFD}\|_{L^2(\Omega)}$ are close in value at both times for $\chi\le 1$. For $\chi=10$, $\|s_{SEM}\|_{L^2(\Omega)}$ is almost twice as bigger than $\|s_{FFD}\|_{L^2(\Omega)}$ at $t=1$, but about the same when $t=0.1$.

Fig. 3 shows $\|s_{SEM}\|_{L^2(\Omega)}$ and $\|s_{FFD}\|_{L^2(\Omega)}$ for $Re=1000$, and 10000 at $t=0.1$, and 1.

The data listed in Tables 6-7 compares the maximum sensitivity via SEM and FFD over the time interval [0,1], i.e., $\|s_{SEM}\|_{L^\infty(0,1;L^2(\Omega))}$ and $\|s_{FFD}\|_{L^\infty(0,1;L^2(\Omega))}$, for $Re=1000$, and 10000 with different χ values as the spatial mesh size is refined. It is worth mentioning that the maximum sensitivity value via both techniques happen at the final time for any mesh size as well as any selected χ values. We have the following observations,

- There is a decrease in $\|s_{SEM}\|_{L^\infty(0,1;L^2(\Omega))}$ and $\|s_{FFD}\|_{L^\infty(0,1;L^2(\Omega))}$ as the spatial mesh size is refined for $\chi\le 1$.
- $\|s_{SEM}\|_{L^\infty(0,1;L^2(\Omega))} < \|s_{FFD}\|_{L^\infty(0,1;L^2(\Omega))}$ for any fixed mesh size as long as $\chi\le 1$.
- For $\chi=10$, $\|s_{SEM}\|_{L^\infty(0,1;L^2(\Omega))}$ values stay close through the mesh refinement, however $\|s_{FFD}\|_{L^\infty(0,1;L^2(\Omega))}$ values increase as the mesh size becomes smaller.
- $\|s_{SEM}\|_{L^\infty(0,1;L^2(\Omega))} > \|s_{FFD}\|_{L^\infty(0,1;L^2(\Omega))}$ for any fixed mesh size with $\chi=10$.

In the next experiment, we consider the natural way of obtaining a measure for accuracy of the approximated velocity solution using different values of parameter χ via

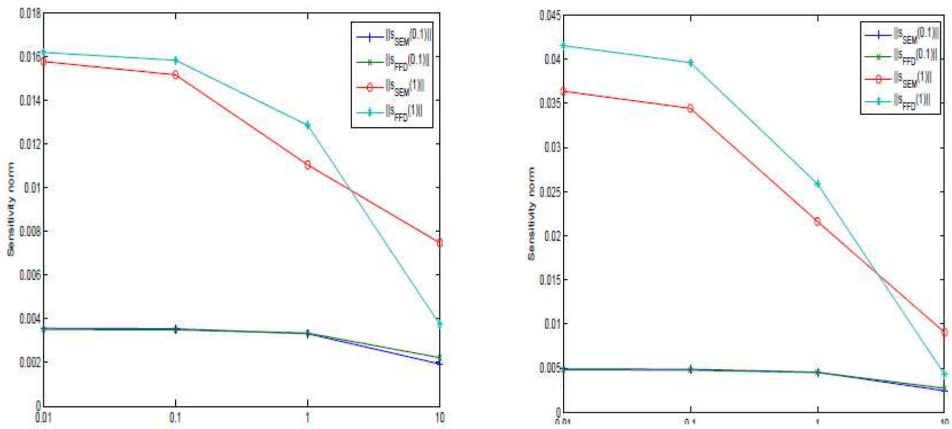

(a) (b)

Figure 3: Sensitivity norms via SEM and FFD for $Re=$ 1000, and 10000 (from (a) to (b)).

Table 6: Sensitivity computations using SEM and FFD for $Re=1000$ with mesh refinement.

χ	Method	$h=\frac{1}{9}$	$h=\frac{1}{18}$	$h=\frac{1}{36}$
0.01	SEM	0.0586237	0.035002	0.0157713
	FFD	0.0599195	0.0356625	0.0161915
0.1	SEM	0.0541932	0.0330563	0.0151647
	FFD	0.0566883	0.0343268	0.015834
1	SEM	0.0250335	0.0199503	0.0110461
	FFD	0.0334313	0.024044	0.0128588
10	SEM	0.00893807	0.00966404	0.00747537
	FFD	0.00131727	0.00297799	0.00373012

Table 7: Sensitivity computations using SEM and FFD for $Re=10000$ with mesh refinement.

χ	Method	$h=\frac{1}{9}$	$h=\frac{1}{18}$	$h=\frac{1}{36}$
0.01	SEM	0.0808053	0.0595574	0.0363773
	FFD	0.109946	0.0778098	0.0415477
0.1	SEM	0.0747136	0.0557121	0.0344382
	FFD	0.10106	0.0722157	0.039622
1	SEM	0.0347436	0.0307948	0.02162
	FFD	0.0475241	0.0389362	0.0258911
10	SEM	0.0094678	0.0106285	0.0090533
	FFD	0.00140832	0.00320407	0.0043209

computing $\chi\|\mathbf{s}\|_{l^2(0,1;L^2(\Omega))}$. The idea is simply based on the following difference quotient for the sensitivity,

$$\mathbf{s}=\frac{\partial\mathbf{u}}{\partial\chi}\approx\frac{\mathbf{u}(\chi)-\mathbf{u}(0)}{\chi},$$

where $\mathbf{u}$ is considered an implicit function of χ. Thus $\mathbf{u}(0)$ indicates the true solution of Navier-Stokes equations while $\mathbf{u}(\chi)$ for $\chi>0$ denotes the corresponding TRM approximation of the velocity.

The last table shows $\chi\|s_{SEM}\|_{l^2(0,1;L^2(\Omega))}$ and $\chi\|s_{FFD}\|_{l^2(0,1;L^2(\Omega))}$ for Reynolds numbers Re=1000,5000, and 10000 with χ=0.01,0.1,1, and 10. As seen in this table, $\chi\|\mathbf{s}\|_{l^2(0,1;L^2(\Omega))}$ values via both methods take larger values for larger Re with any selected value of parameter χ. For $Re=1000$, we suggest $\chi\le 1$ as the best choice of accuracy while for larger Re values, we select a smaller interval of χ values, that is $\chi\le 0.1$. Fig. 4 presents a graphical illustration of data in Table 8.

Remark 5.1. In this experiment, we chose χ values for which $\chi\|\mathbf{s}\|_{l^2(0,1;L^2(\Omega))}\le 0.01$ for the best accuracy. The smaller χ values, the more precise calculations of approximated velocity $\mathbf{u}$ becomes in comparison to the NSE velocity. However, very small values of parameter χ results in increasing the complexity of flow structures/scales that cannot be supported by the grid/mesh and thus numerical pollution of the computed velocity starts. Therefore, the user must consider the trade-off between increased precision and computational flow complexity when choosing the χ value.

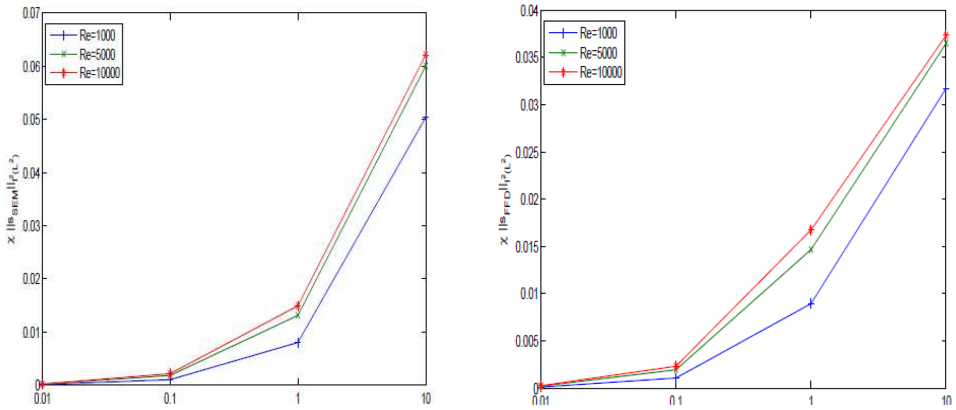

(a) (b)

Figure 4: Sensitivity values, $\chi\|s_{SEM}\|_{l^2(0,1;L^2(\Omega))}$ and $\chi\|s_{FFD}\|_{l^2(0,1;L^2(\Omega))}$ (from (a) to (b)).

Table 8: Sensitivity values using SEM and FFD.

χ		$Re=1000$	$Re=5000$	$Re=10000$
0.01	$\chi\|s_{SEM}\|_{l^2(0,1;L^2(\Omega))}$	0.000106756	0.000191289	0.0002248
	$\chi\|s_{FFD}\|_{l^2(0,1;L^2(\Omega))}$	0.0001075	0.000199557	0.000240192
0.1	$\chi\|s_{SEM}\|_{l^2(0,1;L^2(\Omega))}$	0.00103614	0.00184001	0.00215508
	$\chi\|s_{FFD}\|_{l^2(0,1;L^2(\Omega))}$	0.00105613	0.00193546	0.00231656
1	$\chi\|s_{SEM}\|_{l^2(0,1;L^2(\Omega))}$	0.00803338	0.0131381	0.0149263
	$\chi\|s_{FFD}\|_{l^2(0,1;L^2(\Omega))}$	0.00894438	0.0146596	0.0167499
10	$\chi\|s_{SEM}\|_{l^2(0,1;L^2(\Omega))}$	0.0503827	0.060064	0.0621485
	$\chi\|s_{FFD}\|_{l^2(0,1;L^2(\Omega))}$	0.0317307	0.0365005	0.0373436

5.3 3D Ethier-Steinman problem

This 3D example is defined on the $(-1,1)^3$ domain. In the NSE, the initial condition and the non-homogeneous Dirichlet boundary conditions are selected such that the exact solution (the right hand side function is 0) for this problem [16], is given by

$$
\begin{aligned}
u1 &= -a(e^{ax}\sin(ay+dz)+e^{az}\cos(ax+dy))e^{-\nu d^2 t},\\
u2 &= -a(e^{ay}\sin(az+dx)+e^{ax}\cos(ay+dz))e^{-\nu d^2 t},\\
u3 &= -a(e^{az}\sin(ax+dy)+e^{ay}\cos(az+dx))e^{-\nu d^2 t},\\
p &= -\frac{a^2}{2}(e^{2ax}+e^{2ay}+e^{2az}+2\sin(ax+dy)\cos(az+dx)e^{a(y+z)}\\
&\quad +2\sin(ay+dz)\cos(ax+dy)e^{a(z+x)}\\
&\quad +2\sin(az+dx)\cos(ay+dz)e^{a(x+y)})e^{-\nu d^2 t}.
\end{aligned}
$$

Table 9: Sensitivity in TRM model with the exact solution Ethier-Steinman problem with $a=1.25$, $d=1$ for different Renold number and different χ at $T=0.1$ on the $(-1,1)^3$ domain, where $\Delta t=0.01$, and the mesh size is $h=2/13$.

χ	$Re=1$	$Re=100$	$Re=10000$
0.01	0.015414	0.152852	0.194187
0.1	0.0154026	0.1522	0.193201
1	0.0152893	0.145887	0.183747

The spatial grid size and the filter width are set to be $h=2/13$ and $\delta=h$, respectively. The computations are carried out using the following values of parameters, a=1.25, d=1, final time $T=0.1$, time step $\Delta t=0.01$. The sensitivity is computed via SEM using Taylor-Hood finite elements for $Re=1$,100, and 10000. Sensitivity values listed in Table 9, show that higher Reynolds number yields a higher sensitivity for the given χ values. We notice the same sensitivity behaviour as in the 2D cavity test problem. For all the tested Re values, the sensitivity decreases as χ takes larger values.

6 Conclusions and future directions

Numerical finite element analysis is presented for the SEM method of the TRM model. This is followed by 2D and 3D numerical experiments. We provided a numerical test confirming the rate of convergence for the approximated sensitivity using Taylor-Hood finite elements as well as mini elements Pb1/P1. A numerical comparison between two different methods, SEM and FFD, are performed using the 2D Cavity test problem. Our computations show that the sensitivity norms via both methods are close for $\chi\leq 1$ for all the tested Reynolds numbers, and they increase in the value as time progresses. In addition, we suggested χ values less than one for high Reynolds numbers in order to achieve a better accuracy.

Appendix

In the process of proving Theorem 4.1, we first bound all the terms on the RHS of (4.9) as following,

$$\nu a(\boldsymbol{\eta}^{n+1/2},\boldsymbol{\phi}_h^{n+1/2})\leq\nu\|\nabla\boldsymbol{\eta}^{n+1/2}\|\|\nabla\boldsymbol{\phi}_h^{n+1/2}\|\leq\frac{\nu}{18}\|\nabla\boldsymbol{\phi}^{n+1/2}\|^2+C\nu\|\nabla\boldsymbol{\eta}^{n+1/2}\|^2,$$

$$(r^{n+1/2}-q,\nabla\cdot\boldsymbol{\phi}_h^{n+1/2})\leq\|r^{n+1/2}-q\|\|\nabla\cdot\boldsymbol{\phi}_h^{n+1/2}\|\leq\|r^{n+1/2}-q\|\|\nabla\boldsymbol{\phi}_h^{n+1/2}\|$$
$$\leq\frac{\nu}{18}\|\nabla\boldsymbol{\phi}_h^{n+1/2}\|^2+C\nu^{-1}\|r^{n+1/2}-q\|^2,$$

$$(\boldsymbol{\varepsilon}^{n+1/2}-\overline{\boldsymbol{\varepsilon}}^{n+1/2},\boldsymbol{\phi}_h^{n+1/2})\leq\|\boldsymbol{\varepsilon}^{n+1/2}-\overline{\boldsymbol{\varepsilon}}^{h^{n+1/2}}\|\|\boldsymbol{\phi}_h^{n+1/2}\|$$
$$\leq C(\|\boldsymbol{\varepsilon}^{n+1/2}\|+\|\overline{\boldsymbol{\varepsilon}}^{n+1/2}\|)\|\nabla\boldsymbol{\phi}_h^{n+1/2}\|\leq C\|\nabla\boldsymbol{\varepsilon}^{n+1/2}\|\|\nabla\boldsymbol{\phi}_h^{n+1/2}\|$$

$$
\begin{aligned}
&\le \frac{\nu}{18}\|\nabla \boldsymbol{\phi}_h^{n+1/2}\|^2 + C\nu^{-1}\|\nabla \varepsilon^{n+1/2}\|^2,\\
&\chi(\boldsymbol{\eta}^{n+1/2},\boldsymbol{\phi}_h^{n+1/2}) \le \chi\|\boldsymbol{\eta}^{n+1/2}\|\|\boldsymbol{\phi}_h^{n+1/2}\| \le \frac{\chi}{2}\|\boldsymbol{\phi}_h^{n+1/2}\|^2 + C\chi\|\boldsymbol{\eta}^{n+1/2}\|^2,\\
&\chi(\mathbf{w}^{n+1/2}-\mathbf{w}_h^{n+1/2},\boldsymbol{\phi}_h^{n+1/2}) \le \chi\|\mathbf{w}^{n+1/2}-\mathbf{w}_h^{n+1/2}\|\|\boldsymbol{\phi}_h^{n+1/2}\|\\
&\le C\chi\|\mathbf{w}^{n+1/2}-\mathbf{w}_h^{n+1/2}\|\|\nabla\boldsymbol{\phi}_h^{n+1/2}\|\\
&\le \frac{\nu}{18}\|\nabla \boldsymbol{\phi}_h^{n+1/2}\|^2 + C\nu^{-1}\chi^2\|\mathbf{w}^{n+1/2}-\mathbf{w}_h^{n+1/2}\|^2.
\end{aligned}
$$

All the bounds on the expanded nonlinear terms are given below. Note that $|b^*(\mathbf{u}_h^{n+1/2},\boldsymbol{\phi}_h^{n+1/2},\boldsymbol{\phi}_h^{n+1/2})|=0$,

$$
\begin{aligned}
|b^*(\boldsymbol{\eta}^{n+1/2},\mathbf{u}^{n+1/2},\boldsymbol{\phi}_h^{n+1/2})| &\le C\|\nabla\boldsymbol{\eta}^{n+1/2}\|\|\nabla\mathbf{u}^{n+1/2}\|\|\nabla\boldsymbol{\phi}_h^{n+1/2}\|\\
&\le \frac{\nu}{18}\|\nabla\boldsymbol{\phi}_h^{n+1/2}\|^2 + C\nu^{-1}\|\nabla\mathbf{u}^{n+1/2}\|\|\nabla\boldsymbol{\eta}^{n+1/2}\|,\\
|b^*(\boldsymbol{\phi}_h^{n+1/2},\mathbf{u}^{n+1/2},\boldsymbol{\phi}_h^{n+1/2})| &\le \sqrt{\|\boldsymbol{\phi}_h^{n+1/2}\|\|\nabla\boldsymbol{\phi}_h^{n+1/2}\|}\|\nabla\mathbf{u}^{n+1/2}\|\|\nabla\boldsymbol{\phi}_h^{n+1/2}\|\\
&\le \|\boldsymbol{\phi}_h^{n+1/2}\|^{1/2}\|\nabla\mathbf{u}^{n+1/2}\|\|\nabla\boldsymbol{\phi}_h^{n+1/2}\|^{3/2}\\
&\le \frac{\nu}{18}\|\nabla\boldsymbol{\phi}_h^{n+1/2}\|^2 + C\nu^{-3}\|\nabla\mathbf{u}^{n+1/2}\|^4\|\boldsymbol{\phi}_h^{n+1/2}\|^2,
\end{aligned}
$$

$$
\begin{aligned}
&|b^*(\mathbf{s}_h^{n+1/2},\mathbf{u}^{n+1/2}-\mathbf{u}_h^{n+1/2},\boldsymbol{\phi}_h^{n+1/2})|\\
&\le |b^*(\boldsymbol{\eta}_h^{n+1/2},\mathbf{u}^{n+1/2}-\mathbf{u}_h^{n+1/2},\boldsymbol{\phi}_h^{n+1/2})| + |b^*(\boldsymbol{\phi}_h^{n+1/2},\mathbf{u}^{n+1/2}-\mathbf{u}_h^{n+1/2},\boldsymbol{\phi}_h^{n+1/2})|\\
&\quad + |b^*(\mathbf{s}^{n+1/2},\mathbf{u}^{n+1/2}-\mathbf{u}_h^{n+1/2},\boldsymbol{\phi}_h^{n+1/2})|\\
&\le \frac{\nu}{18}\|\nabla\boldsymbol{\phi}_h^{n+1/2}\|^2 + C\nu^{-1}\|\boldsymbol{\eta}^{n+1/2}\|\|\nabla\boldsymbol{\eta}^{n+1/2}\|\|\nabla(\mathbf{u}^{n+1/2}-\mathbf{u}_h^{n+1/2}\|^2\\
&\quad + C\nu^{-3}\|\nabla(\mathbf{u}^{n+1/2}-\mathbf{u}_h^{n+1/2})\|^4\|\boldsymbol{\phi}_h^{n+1/2}\|^2 + C\nu^{-1}\|\nabla\mathbf{s}^{n+1/2}\|^2\|\nabla(\mathbf{u}^{n+1/2}-\mathbf{u}_h^{n+1/2}\|^2,
\end{aligned}
$$

$$
\begin{aligned}
|b^*(\mathbf{u}_h^{n+1/2},\boldsymbol{\eta}^{n+1/2},\boldsymbol{\phi}_h^{n+1/2})| &\le \sqrt{\|\mathbf{u}_h^{n+1/2}\|\|\nabla\mathbf{u}_h^{n+1/2}\|}\|\nabla\boldsymbol{\eta}^{n+1/2}\|\|\nabla\boldsymbol{\phi}_h^{n+1/2}\|\\
&\le \frac{\nu}{18}\|\nabla\boldsymbol{\phi}_h^{n+1/2}\|^2 + C\nu^{-1}\|\mathbf{u}_h^{n+1/2}\|\|\nabla\mathbf{u}_h^{n+1/2}\|\|\nabla\boldsymbol{\eta}^{n+1/2}\|^2\\
&\le \frac{\nu}{18}\|\nabla\boldsymbol{\phi}_h^{n+1/2}\|^2 + C\nu^{-1}\|\nabla\mathbf{u}_h^{n+1/2}\|\|\nabla\boldsymbol{\eta}^{n+1/2}\|^2,
\end{aligned}
$$

$$
\begin{aligned}
&|b^*(\mathbf{u}^{n+1/2}-\mathbf{u}_h^{n+1/2},\mathbf{s}^{n+1/2},\boldsymbol{\phi}_h^{n+1/2})|\\
&\le \sqrt{\|\mathbf{u}^{n+1/2}-\mathbf{u}_h^{n+1/2}\|\|\nabla(\mathbf{u}^{n+1/2}-\mathbf{u}_h^{n+1/2})\|}\|\nabla\mathbf{s}^{n+1/2}\|\|\nabla\boldsymbol{\phi}_h^{n+1/2}\|\\
&\le \frac{\nu}{18}\|\nabla\boldsymbol{\phi}_h^{n+1/2}\|^2 + C\nu^{-1}\|\mathbf{u}^{n+1/2}-\mathbf{u}_h^{n+1/2}\|\|\nabla(\mathbf{u}^{n+1/2}-\mathbf{u}_h^{n+1/2})\|\|\nabla\mathbf{s}^{n+1/2}\|^2,\\
&\le \frac{\nu}{18}\|\nabla\boldsymbol{\phi}_h^{n+1/2}\|^2 + C\nu^{-1}\|\nabla(\mathbf{u}^{n+1/2}-\mathbf{u}_h^{n+1/2})\|^2\|\nabla\mathbf{s}^{n+1/2}\|^2.
\end{aligned}
$$

Following we obtain all the bounds on the RHS of (4.11)

$$
\Delta t\sum_{n=0}^{N} C\nu\|\nabla\boldsymbol{\eta}^{n+1/2}\|^2 \le C\nu\Delta t\sum_{n=0}^{N+1}\|\nabla\boldsymbol{\eta}^{n+1}\|^2 \le C\nu\Delta t\sum_{n=0}^{N+1} h^{2k}|\mathbf{s}^{n+1}|_{k+1}^2 \le C\nu h^{2k}|||\mathbf{s}|||_{2,k+1}^2,
$$

$$\Delta t\sum_{n=0}^{N} C\chi\|\boldsymbol{\eta}^{n+1/2}\|^2 \le C\chi\Delta t\sum_{n=0}^{N+1}\|\boldsymbol{\eta}^{n+1}\|^2 \le C\chi\Delta t\sum_{n=0}^{N+1} h^{2k+2}|\mathbf{s}^{n+1}|_{k+1}^2 \le C\chi h^{2k+2}|||\mathbf{s}|||_{2,k+1}^2,$$

$$\begin{aligned}\Delta t\sum_{n=0}^{N} C\nu^{-1}\|r^{n+1/2}-q\|^2 &\le C\nu^{-1}\Delta t\sum_{n=0}^{N}\|r^{n+1}-q\|^2 \le C\nu^{-1}\Delta t\sum_{n=0}^{N} h^{2s+2}|r^{n+1}|_{s+1}^2\\ &\le C\nu^{-1}h^{2s+2}|||r|||_{2,s+1}^2.\end{aligned}$$

Based on the error estimate derived in [17], we have

$$\Delta t\sum_{n=0}^{N} C\nu^{-1}\|\nabla(\mathbf{u}^{n+1/2}-\mathbf{u}_h^{n+1/2})\|^2 \le C(\mathbf{u}_0,\mathbf{u},\mathbf{f})\nu^{-2}(h^{2k}+h^{2s+2}+\Delta t^4), \tag{A.1a}$$

$$\begin{aligned}&\Delta t\sum_{n=0}^{N} C\nu^{-1}\chi^2\|\mathbf{w}^{n+1/2}-\mathbf{w}_h^{n+1/2}\|^2\\
&\le C\Delta t\nu^{-1}\chi^2\Big(\sum_{n=0}^{N}\delta^2h^{2k}|\mathbf{s}^{n+1}|_{k+1}^2+\sum_{n=0}^{N}h^{2k+2}|\mathbf{s}^{n+1}|_{k+1}^2+\sum_{n=0}^{N+1}\|\boldsymbol{\eta}^{n+1}\|^2+\sum_{n=0}^{N+1}\|\boldsymbol{\phi}_h^{n+1}\|^2\Big)\\
&\le C\nu^{-1}\chi^2\delta^2h^{2k}|||\mathbf{s}|||_{2,k+1}^2+C\nu^{-1}\chi^2h^{2k+2}|||\mathbf{s}|||_{2,k+1}^2+C\nu^{-1}\chi^2\Big(\Delta t\sum_{n=0}^{N}\|\boldsymbol{\eta}^{n+1}\|^2+\Delta t\sum_{n=0}^{N}\|\boldsymbol{\phi}_h^{n+1}\|^2\Big)\\
&\le C\nu^{-1}\chi^2\delta^2h^{2k}|||\mathbf{s}|||_{2,k+1}^2+C\nu^{-1}\chi^2h^{2k+2}|||\mathbf{s}|||_{2,k+1}^2+C\nu^{-1}\chi^2\Delta t\sum_{n=0}^{N}\|\boldsymbol{\phi}_h^{n+1}\|^2,\end{aligned} \tag{A.1b}$$

$$\begin{aligned}&\Delta t\sum_{n=0}^{N} C\nu^{-1}\|\nabla\mathbf{u}^{n+1/2}\|^2\|\nabla\boldsymbol{\eta}^{n+1/2}\|^2 \le \Delta t\sum_{n=0}^{N} C\nu^{-1}\|\nabla\mathbf{u}^{n+1}\|^2\|\nabla\boldsymbol{\eta}^{n+1}\|^2\\
&\le C\nu^{-1}\Delta t\sum_{n=0}^{N}\|\nabla\mathbf{u}^{n+1}\|^2h^{2k}|\mathbf{s}^{n+1}|_{k+1}^2 \le C\nu^{-1}h^{2k}\Delta t\sum_{n=0}^{N}\|\nabla\mathbf{u}^{n+1}\|^2|\mathbf{s}^{n+1}|_{k+1}^2\\
&\le C\nu^{-1}h^{2k}\Big(\Delta t\sum_{n=0}^{N}\|\nabla\mathbf{u}^{n+1}\|^4\Big)^{\frac12}\Big(\Delta t\sum_{n=0}^{N}|\mathbf{s}^{n+1}|_{k+1}^4\Big)^{\frac12}\\
&\le C\nu^{-1}h^{2k}(|||\nabla\mathbf{u}|||_{4,0}^4+|||\mathbf{s}|||_{4,k+1}^4),\end{aligned} \tag{A.1c}$$

$$\begin{aligned}&\Delta t\sum_{n=0}^{N} C\nu^{-1}\|\boldsymbol{\eta}^{n+1/2}\|\|\nabla\boldsymbol{\eta}^{n+1/2}\|\|\nabla(\mathbf{u}^{n+1/2}-\mathbf{u}_h^{n+1/2})\|^2\\
&\le C\nu^{-1}\Delta t\sum_{n=0}^{N}h^{2k}|\mathbf{s}^{n+1}|_{k+1}^2\|\nabla(\mathbf{u}^{n+1/2}-\mathbf{u}_h^{n+1/2})\|^2\\
&\le C\nu^{-1}h^{2k}\Big(\Delta t\sum_{n=0}^{N}\|\nabla(\mathbf{u}^{n+1/2}-\mathbf{u}_h^{n+1/2})\|^4+\Delta t\sum_{n=0}^{N}|\mathbf{s}^{n+1}|_{k+1}^4\Big)\\
&\le C\nu^{-1}h^{2k}\Big(\Delta t\sum_{n=0}^{N}\|\nabla(\mathbf{u}^{n+1/2}-\mathbf{u}_h^{n+1/2})\|^4+|||\mathbf{s}|||_{4,k+1}^4\Big),\end{aligned} \tag{A.1d}$$

$$\Delta t\sum_{n=0}^{N} C\nu^{-1}\|\nabla\mathbf{u}_h^{n+1/2}\|\|\nabla\boldsymbol{\eta}^{n+1/2}\|^2 \le C\nu^{-1}\Delta t\sum_{n=0}^{N}\|\nabla\mathbf{u}_h^{n+1/2}\|\|\nabla\boldsymbol{\eta}^{n+1}\|^2$$

$$\le C\nu^{-1}\Delta t\sum_{n=0}^{N}\|\nabla\mathbf{u}_h^{n+1/2}\|h^{2k}|\mathbf{s}|_{k+1}^2 \le C\nu^{-1}h^{2k}\Delta t\sum_{n=0}^{N}\|\nabla\mathbf{u}_h^{n+1/2}\||\mathbf{s}^{n+1}|_{k+1}^2$$

$$\le C\nu^{-1}h^{2k}\Big(\Delta t\sum_{n=0}^{N}\|\nabla\mathbf{u}_h^{n+1/2}\|^2+\Delta t\sum_{n=0}^{N}|\mathbf{s}^{n+1}|_{k+1}^2\Big)$$

$$\le C\nu^{-1}h^{2k}\Big(\Delta t\sum_{n=0}^{N}\|\nabla\mathbf{u}_h^{n+1/2}\|^2+\||\mathbf{s}|\|_{2,k+1}^2\Big), \tag{A.1e}$$

$$\Delta t\sum_{n=0}^{N}C\nu^{-1}\|\nabla(\mathbf{u}^{n+1/2}-\mathbf{u}_h^{n+1/2})\|^2\|\nabla\mathbf{s}^{n+1/2}\|^2 \le C\nu^{-1}\Delta t\sum_{n=0}^{N}\|\nabla(\mathbf{u}^{n+1/2}-\mathbf{u}_h^{n+1/2})\|^2$$

$$\le C(\mathbf{u}_0,\mathbf{u},\mathbf{f})\nu^{-2}(h^{2k}+h^{2s+2}+\Delta t^4). \tag{A.1f}$$

We now bound the terms in $Int(\mathbf{s}^{n+1},r^{n+1};\boldsymbol{\phi}_h^{n+1/2})$

$$\Big(\frac{\mathbf{s}^{n+1}-\mathbf{s}^n}{\Delta t}-\mathbf{s}_t(t^{n+1/2}),\boldsymbol{\phi}_h^{n+\frac12}\Big) \le \frac12\|\boldsymbol{\phi}_h^{n+\frac12}\|^2+\frac12\Big\|\frac{\mathbf{s}^{n+1}-\mathbf{s}^n}{\Delta t}-\mathbf{s}_t(t^{n+1/2})\Big\|$$

$$\le \frac12\|\boldsymbol{\phi}_h^{n+\frac12}\|^2+\frac12\frac{\Delta t^3}{1280}\int_{t_n}^{t_{n+1}}\|\mathbf{s}_{ttt}\|^2dt, \tag{A.2a}$$

$$\nu a(\mathbf{s}^{n+1/2}-\mathbf{s}(t^{n+1/2}),\boldsymbol{\phi}_h^{n+\frac12})=\nu(\nabla\mathbf{s}^{n+1/2}-\nabla\mathbf{s}(t^{n+1/2}),\nabla\boldsymbol{\phi}_h^{n+\frac12})$$

$$\le \frac{\nu}{18}\|\nabla\boldsymbol{\phi}_h^{n+\frac12}\|^2+C\nu\|\nabla\mathbf{s}^{n+1/2}-\nabla\mathbf{s}(t^{n+1/2})\|$$

$$\le \frac{\nu}{18}\|\nabla\boldsymbol{\phi}_h^{n+\frac12}\|^2+C\nu\frac{\Delta t^3}{48}\int_{t_n}^{t_{n+1}}\|\nabla\mathbf{s}_{tt}\|^2dt, \tag{A.2b}$$

$$(r^{n+1/2}-r(t^{n+1/2}),\nabla\cdot\boldsymbol{\phi}_h^{n+\frac12}) \le \frac{\nu}{18}\|\nabla\boldsymbol{\phi}_h^{n+\frac12}\|^2+C\nu^{-1}\|r^{n+1/2}-r(t^{n+1/2})\|$$

$$\le \frac{\nu}{18}\|\nabla\boldsymbol{\phi}_h^{n+\frac12}\|^2+C\nu^{-1}\frac{\Delta t^3}{18}\int_{t_n}^{t_{n+1}}\|p_{tt}\|^2dt, \tag{A.2c}$$

$$(\mathbf{u}^{n+1/2}-\overline{\mathbf{u}}^{h^{n+1/2}},\boldsymbol{\phi}_h^{n+\frac12}) \le \frac12\|\boldsymbol{\phi}_h^{n+\frac12}\|^2+\frac12\|\mathbf{u}^{n+1/2}-\overline{\mathbf{u}}^{h^{n+1/2}}\|^2$$

$$\le \frac12\|\boldsymbol{\phi}_h^{n+\frac12}\|^2+C(\delta^2h^{2k}+h^{2k+2})|\mathbf{u}|_{k+1}^2+C\delta^4\|\mathbf{u}\|_2^2, \tag{A.2d}$$

$$(\mathbf{u}(t^{n+1/2})-\overline{\mathbf{u}}(t^{n+1/2}),\boldsymbol{\phi}_h^{n+\frac12}) \le \frac12\|\boldsymbol{\phi}_h^{n+\frac12}\|^2+\frac12\|\mathbf{u}(t^{n+1/2})-\overline{\mathbf{u}}(t^{n+1/2})\|^2$$

$$\le \frac12\|\boldsymbol{\phi}_h^{n+\frac12}\|^2+C\delta^4\|\mathbf{u}\|_2^2, \tag{A.2e}$$

$$\chi(\mathbf{s}^{n+1/2}-\mathbf{w}^{n+1/2},\boldsymbol{\phi}_h^{n+\frac12}) \le \frac{\chi}{2}\|\boldsymbol{\phi}_h^{n+\frac12}\|^2+\frac{\chi}{2}\|\mathbf{s}^{n+1/2}-\mathbf{w}^{n+1/2}\|^2$$

$$\le \frac{\chi}{2}\|\boldsymbol{\phi}_h^{n+\frac12}\|^2+C\chi\delta^4\|\mathbf{s}\|_2^2, \tag{A.2f}$$

$$\chi(\mathbf{s}(t^{n+1/2})-\mathbf{w}(t^{n+1/2}),\boldsymbol{\phi}_h^{n+\frac12}) \le \frac{\chi}{2}\|\boldsymbol{\phi}_h^{n+\frac12}\|^2+\frac{\chi}{2}\|\mathbf{s}(t^{n+1/2})-\mathbf{w}(t^{n+1/2})\|^2$$

$$\le \frac{\chi}{2}\|\boldsymbol{\phi}_h^{n+\frac12}\|^2+C\chi\delta^4\|\mathbf{s}\|_2^2, \tag{A.2g}$$

$$
\begin{aligned}
&b^*(\mathbf{s}^{n+1/2},\mathbf{u}^{n+1/2},\boldsymbol{\phi}_h^{n+\frac{1}{2}})-b^*(\mathbf{s}(t^{n+1/2}),\mathbf{u}(t^{n+1/2}),\boldsymbol{\phi}_h^{n+\frac{1}{2}})\\
&\le b^*(\mathbf{s}^{n+1/2}-\mathbf{s}(t^{n+1/2}),\mathbf{u}^{n+1/2},\boldsymbol{\phi}_h^{n+\frac{1}{2}})+b^*(\mathbf{s}(t^{n+1/2}),\mathbf{u}^{n+1/2}-\mathbf{u}(t^{n+1/2}),\boldsymbol{\phi}_h^{n+\frac{1}{2}})\\
&\le \|\nabla(\mathbf{s}^{n+1/2}-\mathbf{s}(t^{n+1/2}))\|\|\nabla\mathbf{u}^{n+1/2}\|\|\nabla\boldsymbol{\phi}_h^{n+\frac{1}{2}}\|\\
&\quad+\|\nabla\mathbf{s}(t^{n+1/2})\|\|\nabla(\mathbf{u}^{n+1/2}-\mathbf{u}(t^{n+1/2}))\|\|\nabla\boldsymbol{\phi}_h^{n+\frac{1}{2}}\|\\
&\le\frac{\nu}{18}\|\nabla\boldsymbol{\phi}_h^{n+\frac{1}{2}}\|^2+C\nu^{-1}\Delta t^4\|\nabla\mathbf{u}^{n+1/2}\|^4+C\nu^{-1}\Delta t^3\int_{t_n}^{t_{n+1}}\|\nabla\mathbf{s}_{tt}\|^4dt\\
&\quad+C\nu^{-1}\Delta t^4\|\nabla\mathbf{s}(t^{n+1/2})\|^4+C\nu^{-1}\Delta t^3\int_{t_n}^{t_{n+1}}\|\nabla\mathbf{u}_{tt}\|^4dt,
\end{aligned}
\tag{A.2h}
$$

$$
\begin{aligned}
&b^*(\mathbf{u}^{n+1/2},\mathbf{s}^{n+1/2},\boldsymbol{\phi}_h^{n+\frac{1}{2}})-b^*(\mathbf{u}(t^{n+1/2}),\mathbf{s}(t^{n+1/2}),\boldsymbol{\phi}_h^{n+\frac{1}{2}})\\
&\le b^*(\mathbf{u}^{n+1/2}-\mathbf{u}(t^{n+1/2}),\mathbf{s}^{n+1/2},\boldsymbol{\phi}_h^{n+\frac{1}{2}})+b^*(\mathbf{u}(t^{n+1/2}),\mathbf{s}^{n+1/2}-\mathbf{s}(t^{n+1/2}),\boldsymbol{\phi}_h^{n+\frac{1}{2}})\\
&\le \|\nabla(\mathbf{u}^{n+1/2}-\mathbf{u}(t^{n+1/2}))\|\|\nabla\mathbf{s}^{n+1/2}\|\|\nabla\boldsymbol{\phi}_h^{n+\frac{1}{2}}\|\\
&\quad+\|\nabla\mathbf{u}(t^{n+1/2})\|\|\nabla(\mathbf{s}^{n+1/2}-\mathbf{s}(t^{n+1/2}))\|\|\nabla\boldsymbol{\phi}_h^{n+\frac{1}{2}}\|\\
&\le\frac{\nu}{18}\|\nabla\boldsymbol{\phi}_h^{n+\frac{1}{2}}\|^2+C\nu^{-1}\Delta t^4\|\nabla\mathbf{s}^{n+1/2}\|^4+C\nu^{-1}\Delta t^3\int_{t_n}^{t_{n+1}}\|\nabla\mathbf{u}_{tt}\|^4dt\\
&\quad+C\nu^{-1}\Delta t^4\|\nabla\mathbf{u}(t^{n+1/2})\|^4+C\nu^{-1}\Delta t^3\int_{t_n}^{t_{n+1}}\|\nabla\mathbf{s}_{tt}\|^4dt.
\end{aligned}
\tag{A.2i}
$$

Thus,

$$
\begin{aligned}
&\Delta t\sum_{n=0}^{N}\left|Int(\mathbf{s}^{n+1},r^{n+1};\boldsymbol{\phi}_h^{n+1/2})\right|\\
\le&\Delta tC\sum_{n=0}^{N}\|\boldsymbol{\phi}_h^{n+1/2}\|^2+\frac{\chi}{2}\Delta t\sum_{n=0}^{N}\|\boldsymbol{\phi}_h^{n+1/2}\|^2+\frac{\nu}{18}\Delta t\sum_{n=0}^{N}\|\nabla\boldsymbol{\phi}_h^{n+1/2}\|^2\\
&+C\Delta t^4(\|\mathbf{s}_{ttt}\|_{2,0}^2+\nu\|\nabla\mathbf{s}_{tt}\|_{2,0}^2+\nu^{-1}\|p_{tt}\|_{2,0}^2+\nu^{-1}|||\nabla\mathbf{u}|||_{4,0}^4+\nu^{-1}|||\nabla\mathbf{s}|||_{4,0}^4\\
&+\nu^{-1}\|\nabla\mathbf{s}_{tt}\|_{4,0}^4+\nu^{-1}\|\nabla\mathbf{u}_{tt}\|_{4,0}^4)+C(\delta^2h^{2k}+h^{2k+2})|||\mathbf{u}|||_{2,k+1}^2\\
&+C\delta^4|||\mathbf{u}|||_{2,0}^2+C\chi\delta^4|||\mathbf{s}|||_{2,0}^2.
\end{aligned}
\tag{A.3}
$$

References

[1] N. A. Adams and S. Stolz, *Deconvolution methods for subgrid-scale approximation in large eddy simulation,* Modern Simulation Strategies for Turbulent Flow, 2001.

[2] N. A. Adams and S. Stolz, *A subgrid-scale deconvolution approach for shock capturing*, J. Comput. Phys., 178 (2001), pp. 391–426.

[3] M. Anitescu and W. J. Layton, *Sensitivities in large eddy simulation and improved estimates of turbulent flow functionals,* J. Comput. Phys., 178 (2001), pp. 391–426.

[4] M. ANITESCU, F. PAHLEVANI AND W. J. LAYTON, *Implicit for local effects and explicit for nonlocal effects is unconditionally stable,* Electronic Transactions of Numerical Analysis, 18 (2004), pp. 174–187.

[5] J. BORGGAARD AND J. BURNS, *A sensitivity equation approach to shape optimization in fluid flows,* Flow Control, (1995), pp. 49–78.

[6] J. BORGGAARD, J. BURNS, E. CLIFF AND M. GUNZBURGER, *Sensitivity calculations for a 2D, inviscid, supersonic forebody problem,* SIAM, (1993), pp. 14–24.

[7] J. BORGGAARD, D. PELLETIER AND E. TURGEON, *A continuous sensitivity equation method for flows with temperature,* SIAM, (1993), pp. 14–24.

[8] J. BORGGAARD, D. PELLETIER AND E. TURGEON, *A continuous sensitivity equation method for flows with temperature dependent properties,* Proceedings of the 8th A-IAA/USAF/NASA/ISSMO Symposium on Multidisciplanary Analysis and Design, 1993, 2481.

[9] J. BORGGAARD, D. PELLETIER AND E. TURGEON, *Sensitivity and uncertainty analysis for variable property flows*, Proceedings of the 39th AIAA Aerospace Sciences Meeting and Exhibit, 1993, 0140.

[10] J. BORGGAARD AND J. BURNS, *A PDE sensitivity equation method for optimal aerodynamic design,* J. Comput. Phys., 136 (1997), pp. 366–384.

[11] J. BORGGAARD AND A. VERMA, *Solutions to continuous sensitivity equations using automatic differentiation*, SIAM J. Sci. Comput., 22 (2001), pp. 39–62.

[12] J. BORGGAARD AND A. VERMA, *On efficient solutions to the continuous sensitivity equation using automatic differentiation,* SIAM J. Sci. Comput., 22(1) (2000), pp. 39–62.

[13] S. C. BRENNER AND L. R. SCOTT, The Mathematical Theory of Finite Element Methods, Springer-Verlag, 1994.

[14] S. DE, D. HANNASCH, M. NEDA AND E. NIKONOVA, *Numerical analysis and computations of a higher accuracy time relaxation fluid flow model,* Int. J. Comput. Math., (2008), pp. 1–22.

[15] A. DUNCA AND Y. EPSHTEYN, *On the Stolz-Adams deconvolution LES model,* SIAM J. Math. Anal., 2006.

[16] C. EITHIER AND D. STEINMAN, *Exact fully 3d Navier-Stokes solutions for benchmarking*, Int. J. Numer. Methods Fluids, 19 (1994), pp. 369–375.

[17] V. J. ERVIN, W. J. LAYTON AND MONIKA NEDA, *Numerical analysis of a higher order time relaxation model of fluids,* Int. J. Numer. Anal. Model., 4 (2007), pp. 648–670.

[18] A. E. GREEN AND G. I. TAYLOR, *Mechanism of the production of small eddies from larger ones,* Proceeding of Royal Society A, 158 (1937), pp. 499–521.

[19] A. GODFREY AND E. CLIFF, *Direct calculation of aerodynamic force derivatives: a sensitivity equation approach,* Proceedings of the 36th AIAA Aerospace Sciences Meeting and Exhibit, (1998), 0393.

[20] R. GUENANFF, Non-Stationary Coupling of Navier-Stokes/Euler for the Generation and Radiation of Aerodynamic Noises, PhD thesis, Universite Rennes, Rennes, France, 2004.

[21] J. GUERMOND, *Stabilization of Galerkin approximations of transport equations by subgrid modeling,* M2AN, 33 (1999), pp. 1293–1316.

[22] M. GUNZBURGER, Perspectives in Flow Control and Optimization, SIAM publication, 2003.

[23] M. GUNZBURGER, *Sensitivities, adjoints and flow optimization*, Int. J. Numer. Methods Fluids, 31 (1999), pp. 53–78.

[24] B. AVERICK, J. MORE, C. BISCHOF, A. CARLE AND A. GRIEWANK, *Computing large sparse Jacobian matrices using automatic differentiation,* SIAM J. Sci. Comput., 15(2) (1994), pp. 285–294.

[25] A. GRIEWANK, *A mathematical view of automatic differentiation,* Acta Numer., 12 (2003), pp. 321–398.

[26] F. HECHT, O. PIRONNEAU AND K. OSHTSUKA, Software Freefem++, 2003, `http://www.freefem++.org`.

[27] J. G. HEYWOOD AND R. RANNACHER, *Finite element approximation of the nonstationary Navier-Stokes problem, Part IV: error analysis for the second order time discretization,* SIAM J. Numer. Anal., 2 (1990), pp. 353–384.

[28] P. HOVLAND, B. MOHAMMADI AND C. BISCHOF, *Automatic differentiation and Navier-Stokes computations*, Comput. Methods Optimal Design Control, 24 (1998), pp. 265–284.

[29] H. ABDEL-KHALIK, P. HOVLAND, A. LYONS, T. STOVER AND J. UTKE, *A low rank approach to automatic differentiation,* Advances in Automatic Differentiation, 64 (2008), pp. 55–65.

[30] A. LABOVSKY, W. LAYTON, C. MANICA, M. NEDA AND L. REBHOLZ, *The stabilized, extrapolated trapezoidal finite element method for the Navier-Stokes equations*, Comput. Methods Appl. Mech. Eng., 198 (2009), pp. 958–974.

[31] W. LAYTON, Introduction to Finite Element Methods for Incompressible, Viscous Flows, SIAM publications, 2008.

[32] W. LAYTON, C. MANICA, M. NEDA AND L. REBHOLZ, *Numerical analysis of a high accuracy Leray-deconvolution model of turbulence,* Numer. Methods Partial Differential Equations, 24 (2008), pp. 555–582.

[33] W. LAYTON AND L. REBHOLZ, Approximate Deconvolution Models of Turbulence: Analysis, Phenomenology and Numerical Analysis, Springer Lecture Notes in Mathematics, 2012.

[34] W. LAYTON AND M. NEDA, *Truncation of scales by time relaxation*, Technical Report (`www.math.pitt.edu/techrep/0515.pdf`), 2005.

[35] B. LIANG AND S. MAHADEVAN, *Error and uncertainty quantification and sensitivity analysis in mechanics computational models,* Int. J. Uncertainty Quantification, 2 (2011), pp. 147–161.

[36] M. NEDA, *Discontinuous time relaxation method for the time dependent Navier-Stokes equations,* Adv. Numer. Anal., 419021 (2010), pp. 1–21.

[37] MONIKA NEDA AND ELENA NIKONOVA, *Sensitivity computations of time relaxation model with an application in cavity computation,* World Academy of Science, Engineering and Technology, 79 (2011), pp. 542–545.

[38] M. NEDA, F. PAHLEVANI AND J. WATERS, *Sensitvity computations of the Leray-α model,* Contemp. Math. Recent Adv. Sci. Comput. Appl., (2013), 586.

[39] F. PAHLEVANI, *Sensitivity computations of eddy viscosity models with an application in drag computation,* Int. J. Numer. Methods Fluids., 52-4 (2006), pp. 381–392.

[40] F. PAHLEVANI AND L. DAVIS, *Parameter Sensitivity of an eddy viscosity model: analysis, computation and its application to quantifying model reliability,* Int. J. Uncertainty Quantification, 3(5) (2013), pp. 397–419.

[41] P. SAGAUT AND T. LÊ, *Some investigations of the sensitivity of large eddy simulation*, Technical Report (ONERA), 1997.

[42] L. STANLEY AND D. STEWART, Design Sensitivity Analysis: Computational Issues of Sensitivity Equation Methods, SIAM publications, Philadelphia, 2002.

[43] G. I. TAYLOR, *On decay of vortices in a viscous fluid,* Philadelphia Magazine, 46 (1923), pp. 671–674.